NAVAL POSTGRADUATE SCHOOL

MONTEREY, CALIFORNIA

THESIS

THERMOPHOTOVOLTAIC ENERGY CONVERSION IN SUBMARINE NUCLEAR POWER PLANTS

by

John N. Howard

June 2011

Thesis Advisor: Sherif Michael
Second Reader: Todd R. Weatherford

Approved for public release; distribution is unlimited

THIS PAGE INTENTIONALLY LEFT BLANK

REPORT DOCUMENTATION PAGE		Form Approved OMB No. 0704-0188

1. AGENCY USE ONLY *(Leave blank)*	2. REPORT DATE	3. REPORT TYPE AND DATES COVERED
	June 2011	Master's Thesis

4. TITLE AND SUBTITLE Thermophotovoltaic Energy Conversion in Submarine Nuclear Power Plants	5. FUNDING NUMBERS
6. AUTHOR(S) John N. Howard	
7. PERFORMING ORGANIZATION NAME(S) AND ADDRESS(ES) Naval Postgraduate School Monterey, CA 93943-5000	8. PERFORMING ORGANIZATION REPORT NUMBER
9. SPONSORING /MONITORING AGENCY NAME(S) AND ADDRESS(ES) N/A	10. SPONSORING/MONITORING AGENCY REPORT NUMBER

11. SUPPLEMENTARY NOTES The views expressed in this thesis are those of the author and do not reflect the official policy or position of the Department of Defense or the U.S. Government. IRB Protocol number N/A.

12a. DISTRIBUTION / AVAILABILITY STATEMENT	12b. DISTRIBUTION CODE
Approved for public release; distribution is unlimited	A

13. ABSTRACT (maximum 200 words)

Thermophotovoltaic (TPV) cells allow for the direct conversion of infrared (IR) radiation to electricity, similar to when traditional solar cells are exposed to visible light. The objective of this thesis is the development of a computer model of a multijunction TPV cell designed to absorb IR radiation from the primary fluid system of a naval nuclear reactor. This model is then used to determine the feasibility of using this TPV system as a supplemental source of electrical power on a next-generation nuclear submarine. The results of this simulation indicate that the design concept presented in this thesis is a viable option and warrants further consideration and research.

14. SUBJECT TERMS Thermophotovoltaic Cell, Nuclear Fission, Silvaco ATLAS, Modeling, Simulation, Indium Nitride, Indium Gallium Nitride, Indium Arsinide, Multijunction	15. NUMBER OF PAGES 105
	16. PRICE CODE

17. SECURITY CLASSIFICATION OF REPORT	18. SECURITY CLASSIFICATION OF THIS PAGE	19. SECURITY CLASSIFICATION OF ABSTRACT	20. LIMITATION OF ABSTRACT
Unclassified	Unclassified	Unclassified	UU

NSN 7540-01-280-5500 Standard Form 298 (Rev. 2-89)
Prescribed by ANSI Std. 239-18

THIS PAGE INTENTIONALLY LEFT BLANK

Approved for public release; distribution is unlimited

THERMOPHOTOVOLTAIC ENERGY CONVERSION IN SUBMARINE NUCLEAR POWER PLANTS

John N. Howard
Lieutenant, United States Navy
B.S., University of Wisconsin-Madison, 2003

Submitted in partial fulfillment of the
requirements for the degree of

MASTER OF SCIENCE IN ELECTRICAL ENGINEERING

from the

NAVAL POSTGRADUATE SCHOOL
June 2011

Author: John N. Howard

Approved by: Sherif Michael
Thesis Advisor

Todd R. Weatherford
Second Reader

R. Clark Robertson
Chair, Department of Electrical and Computer Engineering

THIS PAGE INTENTIONALLY LEFT BLANK

ABSTRACT

Thermophotovoltaic (TPV) cells allow for the direct conversion of infrared (IR) radiation to electricity, similar to when traditional solar cells are exposed to visible light. The objective of this thesis is the development of a computer model of a multijunction TPV cell designed to absorb IR radiation from the primary fluid system of a naval nuclear reactor. This model is then used to determine the feasibility of using this TPV system as a supplemental source of electrical power on a next-generation nuclear submarine. The results of this simulation indicate that the design concept presented in this thesis is a viable option and warrants further consideration and research.

THIS PAGE INTENTIONALLY LEFT BLANK

TABLE OF CONTENTS

LIST OF FIGURES

THIS PAGE INTENTIONALLY LEFT BLANK

LIST OF TABLES

THIS PAGE INTENTIONALLY LEFT BLANK

LIST OF ACRONYMS AND ABBREVIATIONS

E_g	Bandgap Energy
EM	Electromagnetic
I_{sc}	Short Circuit Current
ICF	Indium Concentration Fraction
InAs	Indium Arsenide
InGaN	Indium Gallium Nitride
InN	Indium Nitride
IR	Infrared
$P_{\max}$	Maximum Power
PV	Photovoltaic
TCAD	Technology Computer Aided Design
TPV	Thermophotovoltaic
V_{oc}	Open Circuit Voltage

THIS PAGE INTENTIONALLY LEFT BLANK

EXECUTIVE SUMMARY

Nuclear power is the standard for electricity and propulsion power production for U.S. submarines. Unfortunately, the overall efficiency of this system, regardless of the advances in reactor design and propulsion technology, is limited due to portions of the system involved in producing and condensing steam. It is becoming more and more difficult to make cost-efficient improvements to the steam cycle to improve the overall power output. Modern photovoltaics (PV), however, are easily exceeding the output efficiencies of the best steam cycles.

The objective of this thesis was to develop a simulation model of a multijunction thermophotovoltaic (TPV) cell that was designed to harness the infrared (IR) radiation given off from the primary fluid system of a nuclear reactor. This model was developed and tested using the ATLAS Virtual Wafer Fabrication suite from Silvaco. The purpose of this model was to determine the feasibility of whether an array of these TPV cells could be used as a supplemental electrical power source for a next-generation nuclear submarine.

PV cells are made from semiconductor materials that undergo the photoelectric effect from certain frequencies of electromagnetic (EM) radiation. The photoelectric effect is the phenomenon where a photon of sufficient energy is absorbed by an electron in an atom. The energy of the photon is converted to kinetic energy of the electron, and the electron departs the atom. This phenomenon is shown in Figure 1 for a material in a vacuum.

In this example, only two of the three incoming photons have sufficient energy to free electrons from the receiving material. It can also be seen in this figure that the excess photon energy is converted into additional kinetic energy and, thus, velocity of the freed electron.

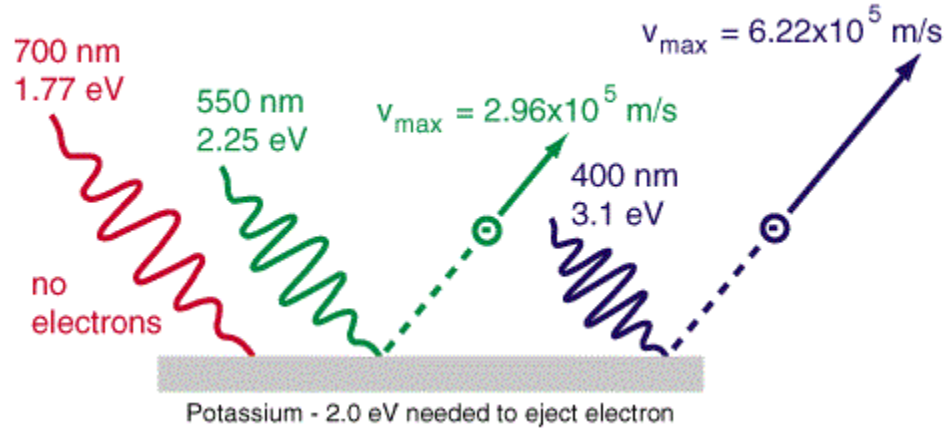

Figure 1. Electrons released after undergoing the photoelectric effect.

This process is somewhat different within a semiconductor material. The amount of energy required to move an electron to the conduction band is known as the material's bandgap energy (E_g) and is represented by the gap between the two bands in Figure 2. Any energy above E_g absorbed by the electron is lost as heat into the crystal lattice of the semiconductor material.

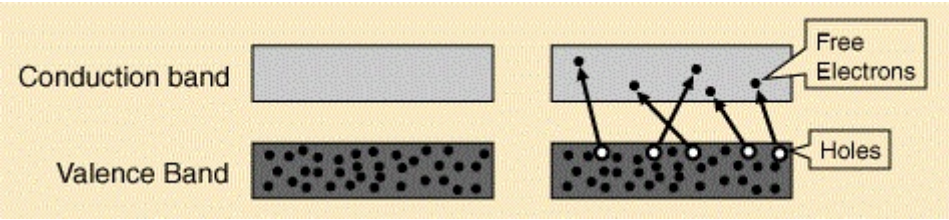

Figure 2. Movement of electrons from the valence band to the conduction band.

TPV cells operate by the same phenomenon except that their E_g is lower, so they can undergo the photoelectric effect from radiation in the IR portion of the EM spectrum. This lower E_g may result in a higher current density than traditional PV materials since lower energy is needed to produce free carriers. However, the voltage produced by TPV materials is lower since there is less of a potential gap for the electrons to overcome.

ATLAS is able to fully design and test a wide range of semiconductor devices, including PV cells. The programmer specifies all the information about the device, from its dimensions and material composition to the incident radiation source and electrical parameters to be tested. This model was designed as three stand-alone layers of the TPV materials Indium Gallium Nitride (InGaN), Indium Nitride (InN), and Indium Arsenide (InAs). Each of these layers is exposed to a radiation spectrum emitted by a blackbody from a range of temperatures. These temperatures, from 500F to 1000F in 100F increments, are intended to model the likely temperatures that would be found from an operating nuclear reactor. The middle and lower layers receive an input spectrum that accounts for the radiation absorbed by the previous layer. The calculations for generating the radiation spectrum files for each blackbody temperature were done in MATLAB. A graph of the spectral radiance vs. radiation wavelength for each of the model temperatures is shown in Figure 2. The vertical lines represent the wavelength equivalents of the bandgap for each of the material layers in the model. A given TPV layer can absorb any radiation whose wavelength is less

than the material's E_g wavelength equivalent. As described above, any energy in excess of the bandgap is lost as heat within the layer.

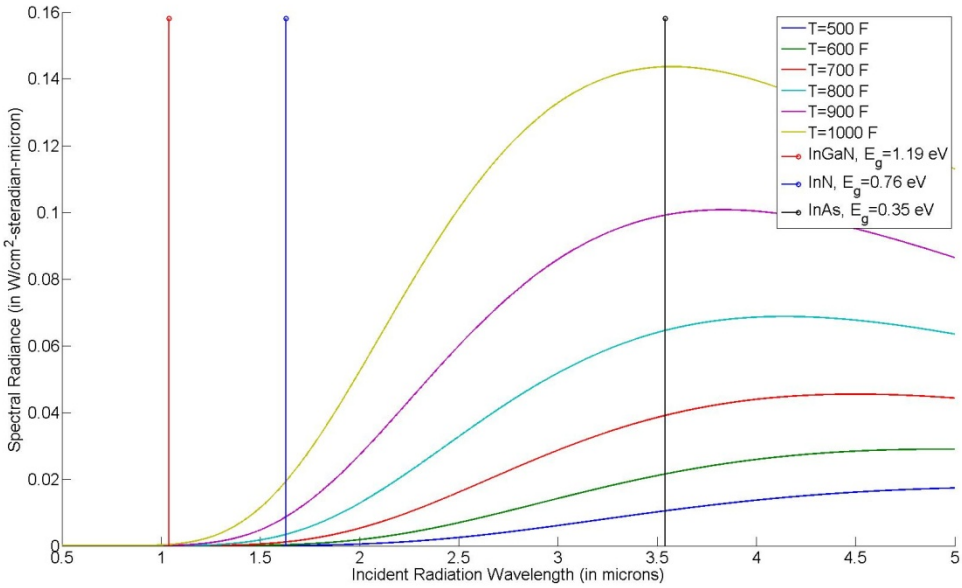

Figure 3. The spectral radiance emitted by blackbodies of varying temperatures and the wavelength equivalents of the bandgap for each material in the model.

The three layers of the model were connected in series within the cell. This affects the electrical output of the cell in two ways. First, the total cell voltage is the sum of the voltages generated by each of the three layers. Second, the total cell current is limited to the smallest value of the maximum current generated by any of the three layers. The current value corresponding to an output voltage of zero is called the short circuit current (I_{sc}), while the voltage value corresponding to an output current of zero is called the open circuit voltage (V_{oc}).

PV cell performance is most commonly viewed through use of a plot of the current vs. voltage known as the I-V

curve. The point of maximum power (P_{max}) is indicated on this graph to show where the product of the current and voltage values is the highest. This P_{max} is used in two ways. First, it is compared to the theoretical maximum power (P_T) which results from the product of I_{sc} and V_{oc}. P_{max} is then divided by P_T and multiplied by 100 to achieve the fill factor as a percentage. This fill factor describes how closely the given layer approaches P_T. The second use of P_{max} is to divide it by the power delivered by the incident radiation and multiply it by 100 to determine the overall efficiency of the cell or any of its layers. The I-V curves for each layer and the combined cell when simulated with a 500F blackbody is shown in Figure 3. The vertical lines in the figure show the P_{max} points for each curve. A similar set of curves was generated for each temperature simulation.

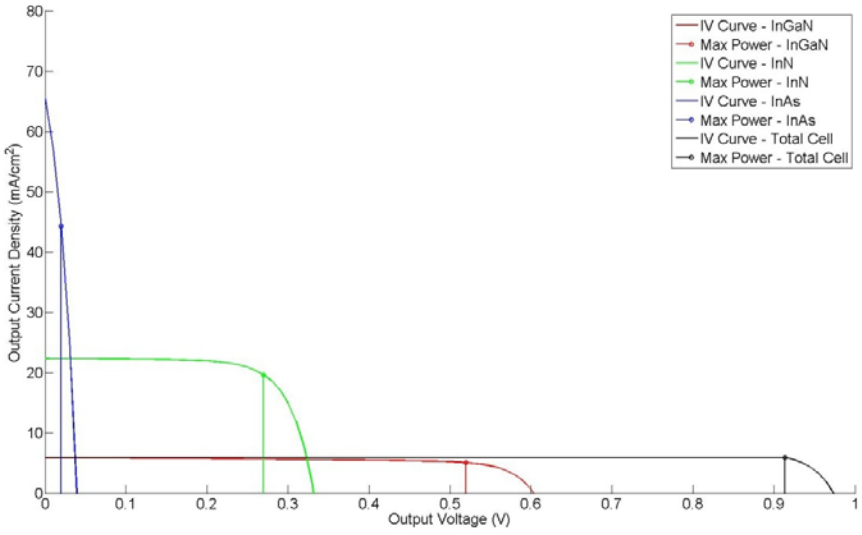

Figure 4. The I-V curves for each layer and the combined cell when modeled at 500F.

The ATLAS simulation produced a set of voltage and current values for each layer of the model. MATLAB was used to process all of this data and determine the performance characteristics for each combined cell at the different blackbody temperatures. The results of the simulation are shown in Table 1.

Table 1. The comparison of TPV cell output at each blackbody radiation temperature.

Blackbody Temperature (F)	**Maximum Current Density (mA/cm^2)**	**Maximum Voltage (V)**	**Maximum Output Power (mW/cm^2)**	**Average Input Power (mW/cm^2)**	**Cell Efficiency (%)**
500	5.9008	0.9139	5.3925	28.7618	18.7489
600	11.1590	0.9699	10.8225	56.3377	19.2101
700	19.0251	0.9796	18.6372	100.1863	18.6026
800	28.7279	0.9847	28.2874	165.3810	17.1044
900	41.3669	1.0152	41.9953	257.4636	16.3112
1000	59.3913	1.0403	61.7859	376.8233	16.3965

Two of the results are worth particular mention. First, without any attempt to optimize the model design, the 600K simulation achieved an efficiency of 19.21%. This is likely due to the given cell parameters being closest to the optimal values for the associated radiation spectrum at that temperature. Second, the 500F simulation returned the

second best efficiency. This lends further weight to the viability of the model as a supplemental power source because 500F is the closest temperature to that at which naval reactors operate today.

The result of this simulation indicates that this model is a viable option as a supplemental power source onboard a nuclear submarine. However, this model is only a small first step and requires additional refinement to provide an accurate description of the real-world performance of this TPV cell.

There are several areas in need of further research. First, the parameters of the cell layers need to be optimized in both thickness and doping concentration to maximize their performance in the expected radiation spectrum of a primary fluid radiator. Second, the incorporation of a specialized semiconductor layer, known a tunnel junction, between the photogenerating layers to make the final cell one monolithic design. The use of a tunnel junction will result in better overall cell efficiency. Third, additional studies should be performed to determine the durability of the materials used in the model when subjected to the radiation fields generated by the fission reaction. Fourth, additional studies should also be conducted to better describe the optical properties of the materials used in this model to improve the simulation accuracy of the model. Fifth, further research should be done to develop advanced PV materials that can generate electricity from the high-energy gamma photons and neutrons emitted by the reactor to further capitalize on available energy sources. Finally, additional work is needed to

determine the effect of using an emitter and filter to shape the radiation spectrum simulated in the model. These two devices can improve the performance of the cell by tailoring and focusing the incident radiation beam at those wavelengths most closely matching the bandgaps of the TPV materials.

There are also several additional applications in which the model developed in this thesis would perform well. First, this system could also supplement nuclear reactors used on aircraft carriers, as well as civilian nuclear power plants, offering a measurable increase in the electrical output of these plants. Second, this TPV cell provides an efficiency that is several times higher than the current thermoelectric conversion options available to space craft utilized for deep space missions. Finally, the advanced PV materials mentioned above could be used to develop a new type of large-scale nuclear battery using spent reactor fuel cores.

The TPV model holds great promise for improving the electricity production capabilities of several different platforms that use nuclear power is some fashion. Even though this model is just the beginning, it clearly demonstrates the potential improvements that are possible with a system of this type.

ACKNOWLEDGMENTS

First and foremost, I would like to thank my wonderful wife, Rosemary. Her love and support throughout the entire process, not to mention her thoughtful and critical discussion of the applications of this work, helped to keep me focused when the road became hard.

I would also like to thank Dr. Sherif Michael for his guidance and support in identifying this topic and helping bring it to life.

Thanks as well to Dr. Todd Weatherford for his assistance in working through my difficulties with the Silvaco program, thus directly contributing to the success of this project.

Finally, I would like to thank Mr. Stephen Bell at Naval Reactors for providing me with his invaluable professional insight into the practical application of this model. His guidance helped to ensure that I presented my findings in such a way as to highlight the realistic value of this design without promising more than the system could deliver.

THIS PAGE INTENTIONALLY LEFT BLANK

I. INTRODUCTION

A. BACKGROUND

Nuclear power has been the standard for producing electrical and propulsion power for American submarines for over 50 years. It is unrivaled for its ability to allow a submarine to operate completely submerged for extended periods of time. However, the design of the most modern nuclear power plant is fundamentally similar to the first steam engine designed over 200 years ago. It still requires a heat source to boil water, and the steam is directed through turbines before being condensed for reuse. There is an upper limit to the cost-effective efficiency improvements that are possible for a heat engine system.

Modern advances in photovoltaic technology have resulted in devices that easily exceed the power output efficiencies of the best heat engine systems. In particular, thermophotovoltaic (TPV) cells can be designed to capture the waste heat produced by large-scale industrial processes (e.g., steel refining and glass making). Similarly, these devices can be designed to operate in support of a nuclear reactor, reducing the need to depend upon power produced solely by steam turbines and helping to improve overall system efficiency.

B. OBJECTIVE

The objective of this thesis is to develop a computer model of a multijunction TPV cell. This model is used to simulate the operation of TPV devices at a variety of temperatures to account for different possible reactor

designs. The model is used to determine the potential power output and conversion efficiency from infrared (IR) radiation. These results help determine the feasibility of using a TPV array to provide some portion of the electrical power for a naval nuclear submarine, which could potentially improve the overall nuclear plant efficiency.

C. RELATED WORK

Several previous researchers at the Naval Postgraduate School developed models of photovoltaic (PV) cells in Silvaco ATLAS. Michalopoulos [1] and Green [2] used ATLAS to model existing PV cells and prove that the simulation results matched closely with published experimental data. Canfield [3] optimized Indium Gallium Arsenide TPV cells for higher operating temperatures. Garcia [4] developed a multijunction PV cell using Indium Gallium Nitride (InGaN).

The focus in this thesis is to develop a model of a TPV cell for the IR radiation fields emitted by a radiator attached to the primary fluid system of a submarine nuclear reactor. It is important for the reader to have a working understanding of the principles that determine the way that TPV cells operate. These fundamental principles are presented in the next chapter.

II. THERMOPHOTOVOLTAIC CELL FUNDAMENTALS

PV cells utilize materials that generate electricity when exposed to sufficient levels of electromagnetic (EM) radiation. These materials come from several different groups on the periodic table of elements. Single element semiconductors come from group IV (e.g., Silicon and Germanium), while *n*-ary (binary, ternary, etc.) semiconductors are most commonly composed of elements found in groups III and V, though recent studies have also looked at the use of elements from groups II and VI.

A. PHOTOELECTRIC EFFECT

The photoelectric effect is a phenomenon wherein a photon of sufficient energy is absorbed by an atom's electron. The photoelectric effect was first observed by Heinrich Hertz in 1887 during his experiments with EM radiation [6]. Numerous scientists over the following years continued to confirm the existence of this effect without coming to a solution for its cause.

The first attempt at explaining the photoelectric effect came in 1902, when Philipp Lenard proposed his triggering hypothesis [6]. This theory stated that electrons in atoms already held a certain amount of potential energy and that incident light only triggered the release of these electrons but did not add any additional energy to them.

In 1905, Albert Einstein developed his competing theory of lightquanta, which held that ordinary light behaved as if it were a stream of individual localized

units of energy [6]. This meant that the frequency of the incident light, when multiplied by Planck's constant, equated to a particular amount of energy. This particular value of energy would only be sufficient to release electrons from certain materials (i.e., vacuum level).

Einstein's theory was eventually proven correct, leading to his receiving the Nobel Prize in Physics in 1921. This award was due in large part to the experimental work of Robert Millikan. Millikan spent several years attempting to provide an experimental determination of the equation Einstein had developed to describe the photo-electric effect. During the course of this work, Millikan also determined the value of Planck's constant to a value very close the theoretical value originally given by Planck. Millikan did not believe that the theory of light-quanta was robust enough to completely discount classical wave theory but might warrant a revision of wave theory [6]. This revision came with the understanding that light can behave as both a particle (i.e., lightquanta) and a wave. It has been firmly established that it is the frequency of light, and not its intensity, that determines whether an electron will be freed from a given material when illuminated.

The equation to determine the energy of the photon is $E_{photon} = h\nu$, where h is Planck's constant (6.626 x 10^{-34} J·s) and ν is the frequency of the incident radiation in Hertz. The energy of the photon is converted into kinetic energy of the electron, thus freeing the electron from its atom. This process is shown in Figure 1 for a material in a vacuum. In this example, only two of the three incoming

photons have sufficient energy to free electrons from the receiving material. It can also be seen in this figure that the excess photon energy is converted into additional kinetic energy and, thus, velocity of the freed electron.

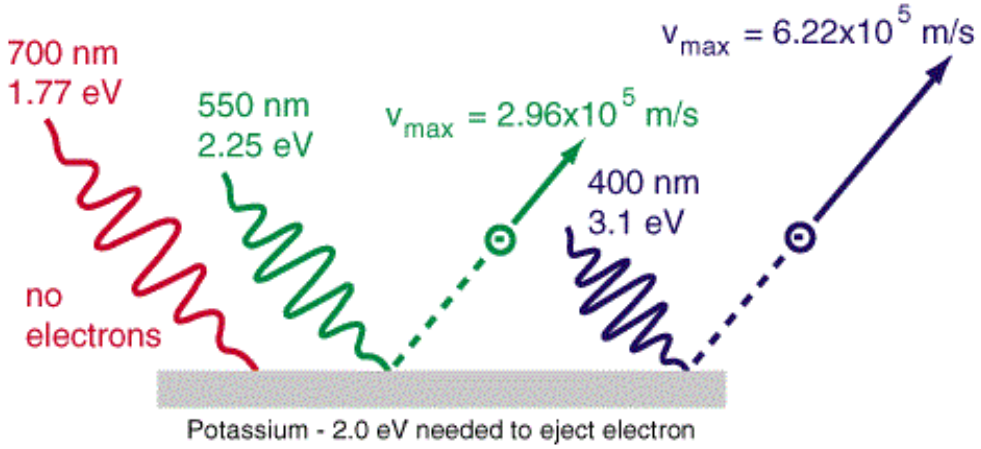

Figure 1. The release of electrons via the photoelectric effect. After [5]

This process is somewhat different within a semiconductor material. The amount of energy required to move an electron to the conduction band is known as the material's bandgap energy (E_g) and is represented by the gap between the two bands in Figure 2. Any energy above E_g absorbed by the electron is lost as heat into the crystal lattice of the semiconductor material. At the same time that an electron is moved to the conduction band, a hole is created in the valence band. These two types of charge carriers are responsible for current flow.

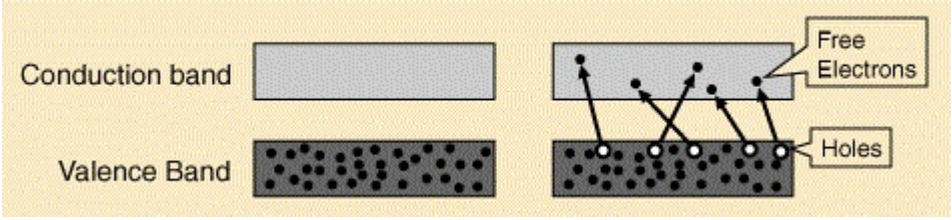

Figure 2. The movement of electrons from the valence band to the conduction band. From [5]

The bandgap of a material also determines the characteristics of how the cell interacts in an electrical circuit. The cell's output voltage is directly related to the material's E_g. The cell's output current is also a function of the bandgap. As E_g lowers, the intrinsic carrier concentration increases, which equates to a lower output resistance for the cell. This means that cells with lower E_g tend to have a higher output current.

B. TPV CELLS

TPV cells are a class of PV cells that are specifically designed to work with photons whose energy levels place them in the IR portion of the EM radiation spectrum. TPV materials necessarily have lower E_g values to absorb the lower energy photons of IR radiation.

Work on TPV cells is thought to have begun in the 1960s and is generally credited to Massachusetts Institute of Technology visiting professor Pierre Aigrain. One of the first applications for this techonology was as a covert power source for the United States Army. These early designs used multifueled burners as the source of IR radiation. General Motors was heavily involved in this

work as an industrial partner to the Army. Both the Army and General Motors terminated their TPV programs in the 1970s. TPV research was almost nonexistent until the solar energy boom in the late 1970s and early 1980s rekindled an interest in this type of device. Private sector research into TPV systems reemerged in the 1990s as several companies began to develop new TPV product designs. The interest in TPV systems within the last decade has generally shifted from the United States to Europe [7].

C. TPV MATERIALS

Three different materials were used in the design of this model. These materials were chosen for their E_g to cover as much of the expected IR radiation spectrum as possible. InGaN, Indium Nitride (InN), and Indium Arsenide (InAs) all have lower E_g and are intended to absorb different portions of the IR radiation.

1. Indium Arsenide

InAs was chosen as the base material for this design primarily for having one of the lowest E_g, currently identified at 0.35 eV. In addition to use in TPV cells, InAs has also seen extensive use in IR lasers and photodetectors.

2. Indium Nitride

InN is a material that is the subject of many ongoing research projects due to both its usefulness as an optical material in the IR portion of the EM spectrum and the controversy regarding its material properties. InN is a

difficult substance to manufacture, and the method of its production seems to have a noticeable impact upon the values of its properties, particularly the value of E_g. Numerous rounds of testing in the 1980s and 1990s seemed to have established a bandgap value of ~1.9 eV based upon sputtering growth techniques. New processes of manufacturing semiconductor devices, called epitaxy, where a given material is layered onto a substrate either as a liquid or a gas, have given rise to higher quality devices. InN devices produced in this way have demonstrated an intrinsic E_g value of around 0.76 eV [8]. The different varieties of epitaxy now seem to be the industry standard, and so a lower E_g value around 0.7 eV has been generally accepted.

3. Indium Gallium Nitride

Like InN, InGaN is a material that has received much attention in recent years. One of the main causes of interest is the variability of the InGaN E_g. The bandgap is determined by the ratio of the concentration of Indium atoms to Gallium atoms. This allows InGaN to absorb EM radiation from the near-IR to the mid-ultraviolet [9]. InGaN is a direct bandgap material, meaning that an electron does not have to absorb extra energy to change its crystal momentum as it moves from the valence to conduction bands. InGaN is often written as $In_xGa_{1-x}N$ or $In_{1-x}Ga_xN$ as a way of describing the given ratio of Indium and Gallium. The bandgap for InGaN is calculated as follows: $E_g(x,T) = (1-x)E_g^{GaN} + xE_g^{InN} - bx(1-x)$, where $E_g^{GaN} = 3.42eV$, $E_g^{InN} = 0.76eV$,

and the bowing parameter $b = 1.44eV$ [9]. The plot of this function, with x ranging from 0 to 1, is shown in Figure 3. The red line in Figure 3 represents the Indium concentration fraction (ICF) for the bandgap that allows for absorption of the uppermost frequency of the IR spectrum. The blue line represents the ICF for the desired E_g of the InGaN layer used in this model.

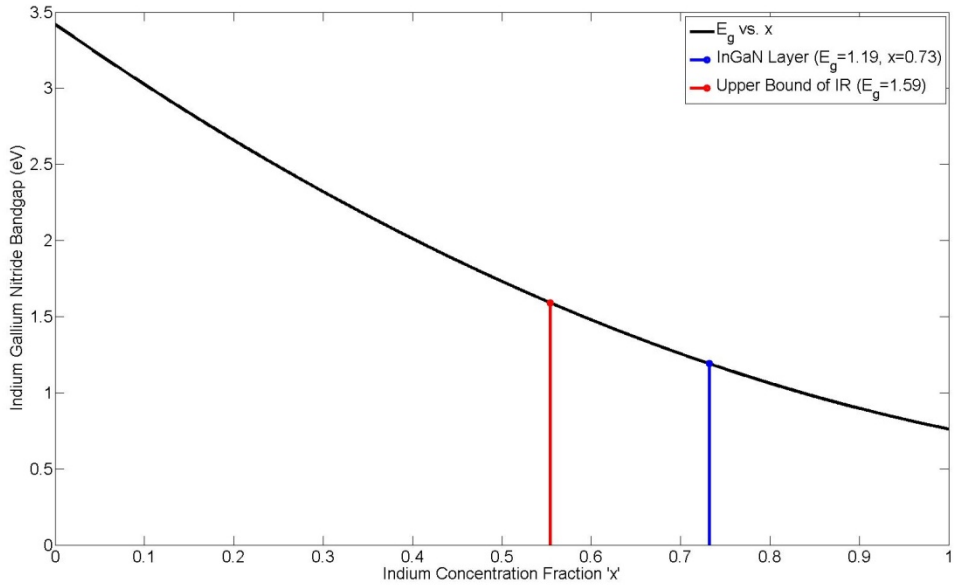

Figure 3. The ICF "x" of InGaN with respect to E_g.

InGaN has also garnered greater interest because of its increased resistance to damage by highly energetic charged particles (e.g., protons, electrons, and alpha particles). Lawrence Berkeley National Laboratory reported that InGaN can be exposed to high-energy charged particle radiation at two to three orders of magnitude greater than other semiconductor materials before showing signs of degradation to its electrical properties [10]. It has been postulated that this radiation resistance is due to the

greater number of structural defects already present in the InGaN lattice, which limits the impact of any further structural damage to a degree not seen in other semiconductor materials.

For many years, engineers and material scientists had to construct a PV cell and test it in a laboratory. They then had to redesign the cell based on those results, build and test the new version, make more revisions, and so on. This was a very resource intensive process that might or might not produce a viable cell design. Nowadays, TCAD programs like ATLAS from Silvaco can design, fabricate, test, and revise PV cells virtually. This results in a more optimal design with a greatly reduced expenditure of time, materials, and finances. The next chapter presents an overview of ATLAS and MATLAB, the two programs used in the development of this model.

III. MODELING AND SIMULATION SOFTWARE

Computer modeling of semiconductor devices, particularly PV cells, has greatly improved the capabilities of engineers to optimize and test their devices. Software-based design avoids the high cost in both materials and time that had previously been associated with the development of improved PV cells. Silvaco's ATLAS technology computer aided design (TCAD) program [11] is used to conduct the simulation and assess the performance of PV cells in this thesis. MATLAB is used to extract pertinent data from the ATLAS output files and determine the electrical operating characteristics of the TPV cell in this model.

A. SILVACO ATLAS

ATLAS is a physically-based two- and three-dimensional device simulator. It predicts the electrical behavior of specified semiconductor structures and provides insight into the internal physical mechanisms associated with device operation [11]. ATLAS is inclusive of several programs that deal with varying aspects of semiconductor design and simulation. The relationship of some of these programs, as well as several of the outputs of ATLAS, is shown in Figure 4.

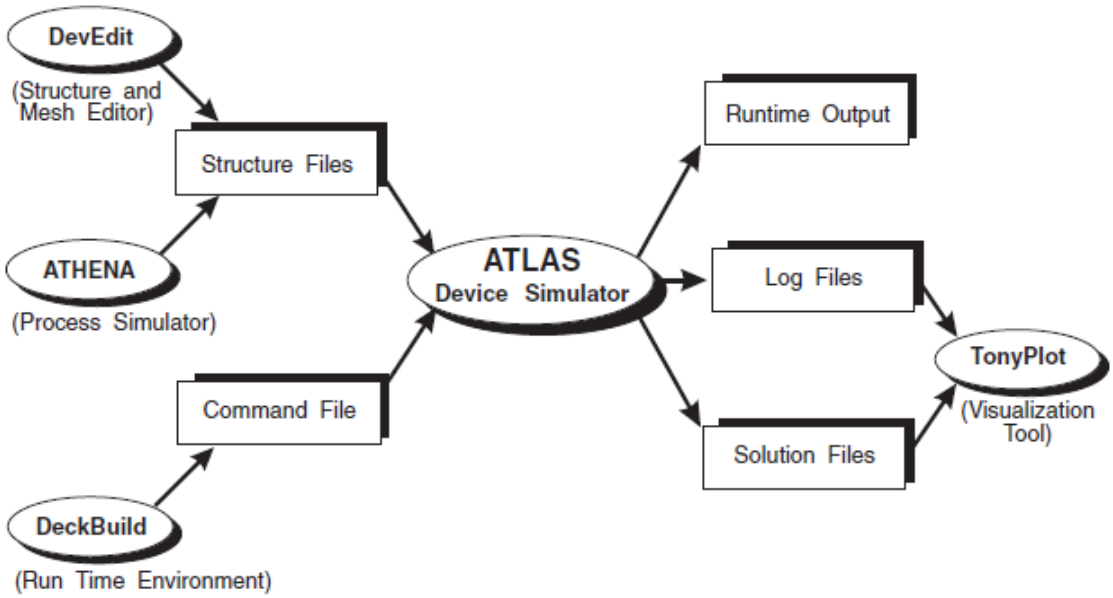

Figure 4. The inputs and outputs of the ATLAS program. From [11]

The DeckBuild program is able to perform all functions of designing and simulating a PV cell and is the sole means of interface used in this thesis. ATLAS takes the cell parameters specified by the designer and generates real-time output of the current status of the simulation. The data resulting from the simulation is saved into standard format log files. DeckBuild has a subroutine called EXTRACT that is capable of providing calculation results regarding cell parameters. However, the author found that using MATLAB made performing these calculations easier, particularly when combining data from different simulation runs.

The log files can also be viewed through TonyPlot, the visual representation program in the ATLAS suite. TonyPlot can generate two- or three-dimensional diagrams of the cell to show physical characteristics (e.g., net doping

concentration) or electrical characteristics (e.g., photogeneration rate). TonyPlot is also able to create line graphs showing the variation of parameters in relation to each other, (e.g., cell output current vs. voltage, cell temperature vs. depth through the cell, etc.).

Each set of code in DeckBuild must begin with the command “go atlas” to activate ATLAS for processing the commands in the rest of the code. ATLAS uses the following format that provides a keyword statement and a set of associated parameters:

<STATEMENT> <PARAMETER>=<VALUE>

The <VALUE> can be one of four types: real, integer, character and logical [11]. An example statement from the ATLAS code in Appendix A is:

material material=Gold real.index=1.2 imag.index=1.8

The <STATEMENT> is “material” and is defined by three <PARAMETER> clauses. The first <PARAMETER> is for “material”, and its <VALUE> is “Gold” and so on for the other two parameters in this line of code. The order of parameters following the statement is arbitrary. Parameters do not have a minimum length of characters other than that they must be uniquely identifiable from other parameters. Any parameter that takes on logical values may be automatically set to “false” by preceding the parameter with the “^” symbol regardless of its default value. A line that begins with a “#” symbol is ignored by the compiler and can be used to create comments within a code. Finally, although DeckBuild can read up to 256 characters

in a single line, the “\” symbol can be used to continue code on the following line for greater readability [11].

ATLAS requires that statements be entered in a particular order to ensure that the program has the correct information to properly simulate the device being designed. Any irregularity in the statement order can cause the program to provide erroneous results or terminate the code altogether. The required order of statement types is shown in Figure 5.

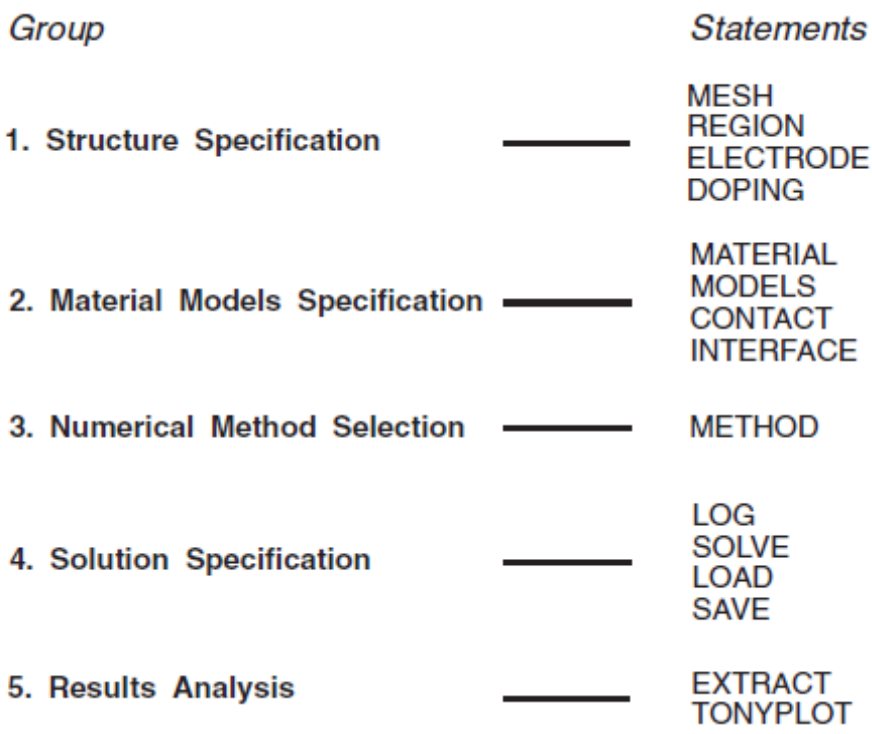

Figure 5. The groups of ATLAS commands and the primary statements made in each group. After [11]

1. Constants

ATLAS allows for the specification of user-defined parameters which can then be assigned as values to standard parameters for defining characteristics of the design cell. This allows for parameters to be much more easily changed during iterative runs of a given design. Standard ATLAS parameters can also be assigned in this way. An example of this type of command is:

```
set cellWidth=500
```

This command defines the horizontal dimension (i.e. x-direction) of the PV cell to be 500 microns, the standard unit of distance in ATLAS. This variable can now be used in other calculations to define other parameters of the cell. An example of the use of this variable is:

```
set cellWidthHalf=$cellWidth/2
```

This cellWidthHalf variable is used later on to define the dimensions of the calculation mesh within the cell. The "$" symbol alerts the code compiler that a previously defined variable is being used. These variables can be altered through the use of a MATLAB script to allow for optimization of a cell's parameters. In particular, the thickness and doping concentration of a given layer within the cell can be iteratively changed to find the ideal values for a given radiation spectrum input.

2. Structure Specification

Once all the user-defined constants are established, the programmer begins defining the structure of the device.

These structural categories are the calculation mesh, the regions, the electrodes, and the doping concentrations of the device.

a. Mesh

The mesh is a series of horizontal and vertical lines throughout the device. Calculations about the electrical characteristics of the device occur at the intersections of these mesh lines. A finer mesh grid provides greater resolution about the performance of the cell but also increases the computational time required to simulate the device. The mesh grid does not have to be uniform throughout the device. If the programmer is interested in a particular portion of the device, the mesh can be made finer in that area, while the remaining mesh is made coarser to reduce the amount of time required to simulate the cell.

The mesh is defined in the x- and y-directions using the following statements:

```
x.mesh location=<VALUE> spacing=<VALUE>
...
y.mesh location=<VALUE> spacing=<VALUE>
...
```

ATLAS also has the ability to automatically define mesh points for a device. This is useful if a programmer is interested in the performance of a device as a whole but

does not need specific information regarding any particular area within the device. An example of using automatic meshing is:

```
mesh width=$zwidth auto
```

In this example, the auto statement allows ATLAS to determine uniform mesh spacing in the y-direction based on the regions that the programmer defines for the device [11]. The programmer must still specify mesh spacing in the x-direction using the defining statement above. The "width=$zwidth" portion of the statement provides an additional dimension to the simulation. As a default, ATLAS assumes that the z-direction dimension of any device is one micron. This dimension can be modified by defining the "width" parameter. Since PV cells are normally compared in terms of per square centimeter output, the output for a 1 cm^2 PV cell can be achieved by defining "width" as a value equal to $1x10^8$ μm^2 divided by the cell width in microns.

A partial view of the mesh defined for the InGaN layer of this model is shown in Figure 6. The view presented is of the air gap from the top of the display down to 0.5 microns, the square cathode in the center, the thin window and emitter layers, and the base region down to one micron.

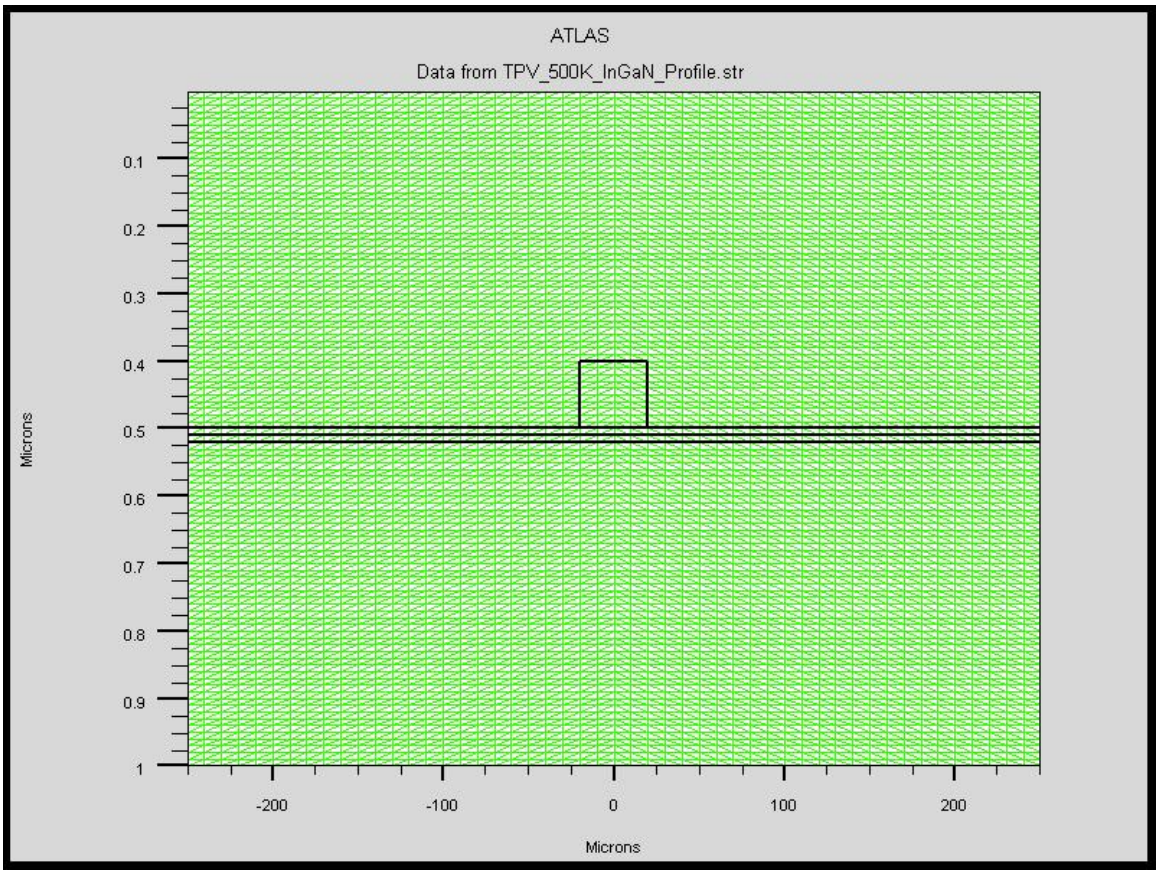

Figure 6. The mesh grid for the upper portion of the InGaN model layer.

b. Regions

The next step in the process of defining a device is to specify the different regions, including the type of material used and the region's dimensions. A standard region statement is given by:

region number=<integer> <material type> \

<position parameters>

The <material type> statement simply assigns a particular material to this region. The properties of this material can be modified later on in the material models section. The <position parameters> provide the x- and y-direction

boundaries for the given region of the device. ATLAS is also able to define structures in terms of cylindrical coordinates to more easily define non-rectangular devices. ATLAS can accommodate up to 200 different regions in a single design. If a material has variable properties based on a specified mole fraction, then that composition fraction is specified within the region statement using the x.comp and y.comp statements. Every portion of the device that has a mesh grid assigned must also have a region statement covering those dimensions [11].

c. Electrodes

The next step is to define the electrical contacts for the device. Each device must have at least one electrode in contact with semiconductor material, and ATLAS can accommodate up to 50 electrodes. The electrode is defined as:

```
electrode name=<electrode name> \
     <position parameters>
```

The electrode can be given any character name (i.e., cathode, anode, gate, etc.), and any electrodes that share the same name are assumed to be electrically connected. The position parameters use the same coordinate system as was used to define the regions.

Single-layer PV cells only need to have two electrodes, anode and cathode, defined for each cell. Multijunction cells using tunnel junctions also need an electrode for each tunnel junction present. Though ATLAS allows for the use of several different metals for electrodes, gold is most commonly used due to its excellent

electrical and thermal properties. The cathode size must be kept small enough to minimize the shadowing effect of blocking EM radiation to the cell while not being too small so as the limit the amount of current flow that it can allow. An optimum size for the cathode width should be eight to ten percent of the width of the cell. The anode covers the entire bottom surface of the cell and is usually modeled as being infinitesimally thin (i.e., its maximum and minimum y-dimensions are the same).

d. Doping

The last of the structural specifications to be made is the doping profile of the device. The doping statement is:

```
doping <distribution type> <dopant type> \
    <position parameters>
```

ATLAS provides three different distribution types: uniform, Gaussian, and complementary error function [11]. The uniform distribution takes the given doping concentration and spreads it evenly throughout the area specified. The Gaussian distribution places the peak concentration along an axis specified by the programmer, and the concentration diminishes according to a traditional Gaussian statistical distribution. The complementary error function distribution takes several inputs into an integral function to give the programmer greater control over the dopant distribution within a region. The dopant type variable defines whether the material is n- or p-type semiconductor material. The position parameters follow the same scheme as the regions previously defined.

3. Material Models Specification

The material models group includes commands for specifying the characteristics of the materials used in the model, the numerical models used to calculate the cell performance, the characteristics of the electrical contacts, and to further define the properties between the interface of semiconductor and insulator materials.

a. Materials

ATLAS is able to simulate semiconductors, insulators, and conductors in the design of a cell. These material properties can be changed from their default values by using a material statement. These statements can be made in one of three ways: by type of material, by region number, or by region name. A statement for each of these is:

```
material material=<character name> \
     <property name>=<VALUE>
material region=<integer> <property name>=<VALUE>
material name=<character name> \
     <property name>=<VALUE>
```

ATLAS has a long list of material properties that can be modified as well as numerous tables of properties for the many materials it can simulate [11].

b. Models

Physical models define how the simulation should expect the model materials to react and interact. These models are grouped into five categories: mobility,

recombination, carrier statistics, impact ionization, and tunneling [11]. The impact ionization category is specified using the "impact" statement, while the other categories are specified using the "models" statement. The models can be specified for use in the entire design or for specific materials through the following two statements:

```
models <model flag> <general properties> \
      <model dependent properties>
models material=<material> <model name> \
      <model properties>
```

The models chosen must be based upon the type of materials being used, the purpose of the device, and the structure of the device. A brief description of the models used in this thesis is provided in Table 1.

Table 1. Brief description of physical models used in this thesis. After [11]

Model Name	**ATLAS Syntax**	**Explanation**
Shockley-Reed-Hall	SRH	Uses fixed minority carrier lifetimes. Should be used in most simulations.
Bandgap Narrowing	BGN	Important in heavily doped regions.
Operating Temperature	TEMPERATURE	Specifies the device temperature in Kelvin.
Model Status	PRINT	Prints the status of all models, a variety of coefficients, and constants.

c. Contacts

The contacts implemented in ATLAS are assumed to be ohmic. If a particular design uses a Schottky contact, the workfunction for that contact must be specified. Any parameters that are different from the default specifications based upon the contact material can also be entered using the following statement:

contact name=<character name> <parameter>

Contact statements can also be used to specify external circuit components (e.g., resistors, capacitors, or inductors) whose effect should also be included in a given simulation [11]. Designs whose simulation does not require modified electrical contact properties do not need to include contact statements.

d. Interfaces

The interface statement is used to define the interface charge density and surface recombination velocity at interfaces between semiconductors and insulators [11]. Such parameters are defined in the program as follows:

interface <parameter>=<VALUE>

Contact between semiconductor and insulator materials are not simulated in this thesis, and so interface statements are not used.

4. Light Beam Specification

PV cell designs require a light source to be specified. The beam statement allows the programmer to define all aspects of the light source. The light source code from this model is as follows:

```
beam num=1 x.origin=0 y.origin=$lightY angle-90 \
     power.file=BBRad500K.spec wavel.num=2251 \
     back.refl
```

This statement begins by describing the position and angle of incidence of the light source in relation to the surface of the cell. The power.file statement loads a separate file that provides spectral intensity data and the associated wavelengths. The wavel.num statement determines how many wavelengths will be evaluated by the simulation. The back.refl statement specifies that back side reflections are to be taken into account [11].

5. Numerical Method Selection

ATLAS utilizes several different numerical solution methods dependent upon the particular device being simulated. The three primary methods used are Gummel (decoupled equations), Newton (fully coupled equations), and Block (mixed coupling equations) [11]. Method statements are made as follows:

```
method <method name> <method parameters>
```

Newton is the default method for simulations incorporating basic drift diffusion of charge carriers, while Gummel tends to provide better initial solutions for simulations. Method parameters provide limitations for the calculations, including aspects like the number of iterations allowed without reaching convergence or the maximum allowed potential update per iteration [11]. A programmer can also use more than one method, as seen in the following example:

```
method gummel newton
```

The benefit to using both methods is that if Gummel fails to converge to a solution, ATLAS switches to the Newton method to achieve a solution. This is a more robust but also more time consuming way of obtaining solutions for any device [11].

6. Solution Specification

The solution specification section cover four different command types for generation and recording of simulation data: log, solve, load, and save.

a. Log

The log command specifies a file to which ATLAS stores all the terminal characteristics generated by any subsequent solve statements [11]. The desired log file is specified by the following:

log outfile=<file name> <output parameters>

ATLAS generates a default set of information from a given simulation. The programmer can add additional parameters to the log statement to ensure that specific data is included in the log file.

b. Solve

The solve command instructs ATLAS to perform a solution for one or more specified bias points [11]. The solve statements remember the results of previous solve statements and incorporate those previous results into the solution of the current iteration. As an example:

solve b1=1.0

solve name=anode vanode=0.0 vstep=0.01 vfinal=1

The first line directs ATLAS to solve for the PV cell's characteristics when exposed to beam 1 at its standard strength. The second line determines the current and voltage results of the cell when the anode voltage is increased from 0 to 1 volt in 0.01 volt increments. These results are stored in any previously specified log file or can be subsequently saved using a save statement. A good initial solution needs to be determined prior to the use of any solve statements whose data is required by the programmer.

c. Load

The load command inputs previous solutions from the specified file as initial guesses to other bias point calculations [11]. The load statement is entered as follows:

load <ASCII/MASTER> <file name>

The first parameter listed instructs ATLAS as to whether the data file being loaded was saved in the ATLAS default MASTER binary format or in a generic ASCII format. The name of the file to be loaded is specified in the second parameter.

d. Save

The save command saves all node point information into a specified output file [11]. The format for the save command is:

save outfile=<file name> <MASTER>

The file to receive the output data can be of any type but is most often saved in the *.log or *.txt format to make

data extraction from the file easier. The MASTER parameter can be included to force the data to be written into the output file in the standard ATLAS format, which also allows the output file to be loaded into TonyPlot for graphical representation.

7. Results Analysis

The results of the ATLAS calculations can be viewed in real-time through the use of extract statements or can be viewed through two- or three-dimensional plots in TonyPlot.

a. Extract

Extract statements display the specified parameters in the run-time output of DeckBuild and can also perform user-defined calculations. Extract statements use the data generated by any previous solve statements or device structure information but can also be given a particular data file to process as follows:

extract initial infile=<file name>

Once this data file has been loaded, subsequent extract statements can display any information or calculations based upon the contents of that file.

In addition to being displayed in the run-time output, the results of extract statements are also saved to a default file called results.final [11]. This output file can be changed using the following statement:

extract ... datafile=<file name>

A given extract data file can be used for several extract statements, or each statement can be assigned its own data file.

b. TonyPlot

TonyPlot is the graphical program used to display the results of ATLAS simulations. The tonyplot statement will start the TonyPlot program and display the information in the specified file [11]:

tonyplot <file name>

TonyPlot can read several different file types, but structure (*.str) and log (*.log) files are the two most common. Loading a structure file into TonyPlot results in a two-dimensional representation of the simulated device. This figure can then be manipulated to show different information about the device (i.e., doping concentration, temperature, photogeneration rate, etc.). Loading a log file generates a line plot of the information included in the log file.

8. Model ATLAS Code

The DeckBuild source code used in this thesis is contained in Appendix A. Since the author simulated the performance of the three TPV layers at six different temperatures, only the code associated with the 500K simulation has been included. The only changes from one temperature version to another are the names of the data output files and the name of the radiation spectrum input file; all other parameters remain the same through all versions of the code. The code files are organized exactly as listed in Figure 4 except that the author defined a number of constants at the start of the file and did not

use any load, extract, or tonyplot statements. All data extraction and manipulation was done with code scripts in MATLAB.

B. MATLAB

MATLAB was utilized in this research as a matrix manipulation software and was used to extract data from the output files generated by ATLAS to calculate system performance parameters. Other researchers at the Naval Postgraduate School have written scripts that allow MATLAB to start Deckbuild, load and simulate device programs, and make changes to the ATLAS code as an iterative means of optimizing the device performance. Canfield [3] improved previous versions of MATLAB scripts to allow for two ATLAS parameters to be optimized concurrently. The MATLAB code used to extract and manipulate the data resulting from ATLAS simulations is contained in Appendix B. MATLAB was also used to generate the input radiation spectrum files for each material layer in this thesis.

ATLAS and MATLAB are both robust and capable programs. They can be used together to complement each other very well, resulting in a more optimal model. The next chapter explains the details of how these programs were used to conduct a feasibility study on a multijunction TPV cell for use with a naval nuclear reactor.

THIS PAGE INTENTIONALLY LEFT BLANK

IV. MODELING OF MULTIJUNCTION THERMOPHOTOVOLTAIC CELLS IN SUPPORT OF A SUBMARINE NUCLEAR REACTOR

Modeling a device using a TCAD simulation program like ATLAS brings inherent questions about the accuracy of the model. The only way establish to the validity of a model is to compare it to results of real-world device operations. As related in Section C of Chapter I, several previous students at the Naval Postgraduate School conducted their thesis work on the verification of ATLAS at a tool for modeling PV cells. Their work helped to confirm the viability of ATLAS as an accurate means of simulating PV cells. This allowed the author to develop a new type of TPV cell model and trust that the results would be representative of a real-world device.

Modern TPV converters consist of more components than just the TPV cell array. A basic example of such a converter is shown in Figure 7. The model in this thesis considers only two of the components shown in this design. The thermal radiator is simulated as a blackbody at the associated temperature. The TPV array is modeled in ATLAS and exposed to the radiation emitted by the blackbody. This model does not consider the use of a filter to allow only discrete wavelengths of IR radiation to reach the TPV cell. This model also does not consider the use of an emitter assembly to increase the spectral intensity of the IR radiation by focusing the radiation beams incident to the TPV cell.

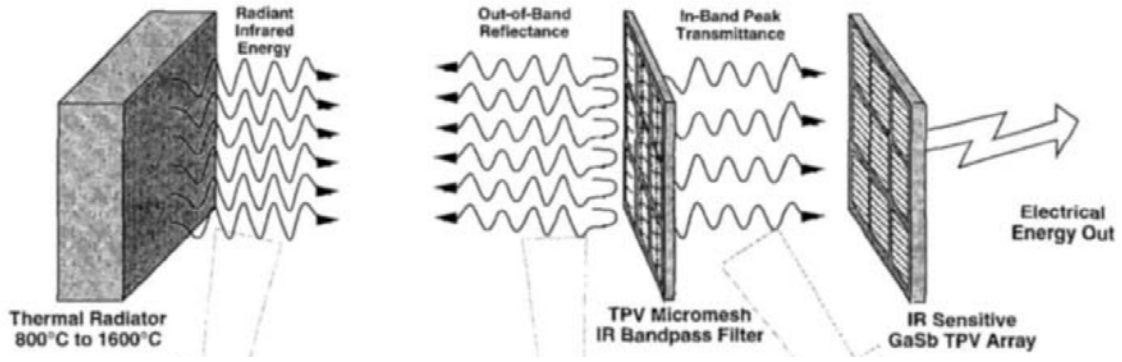

Figure 7. The primary components of a filtered TPV converter. After [12]

A. TPV CELL CONSTRUCTION

The TPV cell designed in this thesis is a multijunction cell but operates as three separate layers as opposed to one monolithic device. This arrangement makes simulation easier for a variety of reasons. Constructing a monolithic PV cell takes a great deal of coordination in matching materials to minimize the instabilities incurred by crystalline lattice mismatch between different materials. Monolithic devices also require the use of either insulating materials between photogenerating layers or highly-doped semiconductor layers called tunnel junctions. The disadvantage to using insulating materials is that the software model must also account for the diffraction and reflection that occur as incident radiation passes through these materials. Tunnel junctions are an advantageous addition to a multijunction cell and can help to improve the overall efficiency of the cell. Unfortunately, they also require a great deal of effort to match to the two layers they connect. Given that the intent of this model is to determine the feasibility of

using a TPV cell array with a nuclear reactor, it is unnecessary to develop a monolithic cell at this point.

1. TPV Cell Layers

The model in this thesis consists of three standalone TPV layers. The materials for these layers were chosen so that their bandgap was evenly distributed across the IR radiation spectrum. One of the primary concerns of using a simulation program is ensuring that the correct values of the material properties are used. ATLAS has an extensive database of material properties available for use, though these values are not always current to ongoing material research. For example, the bandgap for InN is still listed as 1.9 eV, though its value has since been proven to be in the vicinity of 0.7 eV [8]. The values for properties such as this can be modified with material statements in the ATLAS code. Another property that required modification from the ATLAS database was the bandgap of InGaN. The bandgap was calculated as described in Section C.3 of Chapter II. Some of the properties of great concern to the accuracy of this model are the optical indices for each of the materials used.

a. InAs Optical Properties

In addition to the databases of physical and electrical properties, ATLAS also includes a separate database of optical properties supplied by the SOPRA company, a thin film metrology company, that accounts for the temperature and composition of the material under consideration. The author used the SOPRA database entry to supply the optical index values for InAs.

b. InN Optical Properties

Due to the relatively recent interest in the inclusion of InN into PV and TPV devices, detailed information on its properties is still hard to come by. The refractive index and extinction coefficient values used in this model come from a study in 2002 [13]. Unfortunately, these values were determined based on the understanding of the E_g of InN to be 1.9 eV. The author acknowledges that combining these older optical values with the new E_g value does not provide a truly accurate model of the performance of the InN layer but believes that a rough estimation of the layer's performance can be considered until more complete optical data can be utilized.

c. InGaN Optical Properties

InGaN is another material, similar to InN, whose optical properties are relatively unknown due to a lack of extensive research. The author had even more difficulty finding data to support values for the refractive index and extinction coefficients for InGaN. The refractive index value is an approximation based upon data presented in [14]. The extinction coefficient value is an estimate based upon a relation the author noted between the index values of other materials. The sum of the two values is consistently between 3.1 and 3.3. Based upon this, the author chose a value for the extinction coefficient that would add to 3.2 with the approximated value for the refractive index. Again, the author acknowledges that such uncertainty in these parameters limits the accuracy of this

model but believes that the layer's performance can still be considered for determining whether further research on this topic is warranted.

d. Heat Production and Dissipation

Another aspect of the model that differs from real-world behavior is the heating effect of excess photon energy on the TPV material layers. As discussed in Chapter II, Section A, any energy absorbed by an electron that is greater than the material's E_g is lost as heat into the crystal lattice. This heating effect can have a significant impact on the physical and electrical properties of the given material and adversely affect the operation of the TPV cell.

This model does not consider the heating of the crystal lattice. The simulation maintains the entire layer at exactly the temperature specified in the simulation code. A method to limit the heat generated within the cell is the use of input spectrum filters. These filters reflect away photons whose wavelengths and, thus, energy levels are not sufficiently close to the bandgap of the given material. This helps reduce the amount of radiation that can be absorbed in the material that would then produce unwanted heating of the crystal lattice.

2. TPV Cell Electrical Connections

The layers of the TPV cell are electrically connected in series, which affects the output values in two ways. First, the cell output voltage is the sum of the voltages from each of the individual layers. Second, the cell

output current is limited to be no greater than the smallest maximum current of any of the layers.

The current when the anode voltage is zero is called the short circuit current (I_{sc}) and is the largest current value that can be supplied by the layer. Similarly, the anode voltage when the output current is zero is called the open circuit voltage (V_{oc}) and is the largest possible voltage for the layer. These two values define the bounds of the operation of the TPV cell. The values for current and voltage were multiplied together to calculate the power supplied by each cell layer. The maximum power ($P_{\max}$) was recorded out of this data set as well as the associated current and voltage values.

Fill factor is a parameter that is commonly used to determine PV cell performance. Fill factor is calculated by $FF = \frac{P_{\max}}{I_{sc}V_{oc}} \times 100$, where 100 converts fill factor to a percentage. Fill factor corresponds to how closely the $P_{\max}$ approaches the theoretical maximum power achieved by multiplying I_{sc} and V_{oc}. The efficiency of the cell is determined by $\eta_{TPV} = \frac{P_{\max}}{P_{in}} \times 100$, where P_{in} is the power supplied by the blackbody radiation source and 100 converts efficiency to a percentage.

The individual TPV cells are then connected into strings in an array to provide an overall electrical output. Each string supplies a voltage that is the sum of each of the individual cell voltages, and the current is limited to the lowest current supplied by any of the cells.

These strings are then connected together in series and parallel to achieve the desired current and voltage output for the array as a whole.

B. RADIATION SOURCE MODEL

This model simulates a radiator attached to the primary fluid piping of a nuclear reactor as the source of the IR radiation being converted to electricity. This simulation is achieved by treating the radiator as a blackbody radiating at the given temperature. The blackbody spectral intensity is calculated from $L_\lambda = \frac{2x10^{24}hc^2}{\lambda^5}\frac{1}{e^{10^6 hc/\lambda kT}-1}$ [15], where h is Planck's constant (6.626 x 10^{-34} J·s), c is the speed of light in a vacuum (2.998 x 10^8 m/s), λ is the radiation wavelength in microns, k is Boltzmann's constant (1.381 x 10^{-23} J/K), and T is the blackbody temperature in Kelvin. The spectral radiance at each wavelength for each of the six blackbody temperatures is shown in Figure 8. It can be seen that as temperature increases, the peak spectral intensity rises and shifts toward the shorter wavelengths. The red, blue, and black vertical lines in Figure 8 represent the equivalent wavelengths of the E_g for each of the materials used in this thesis.

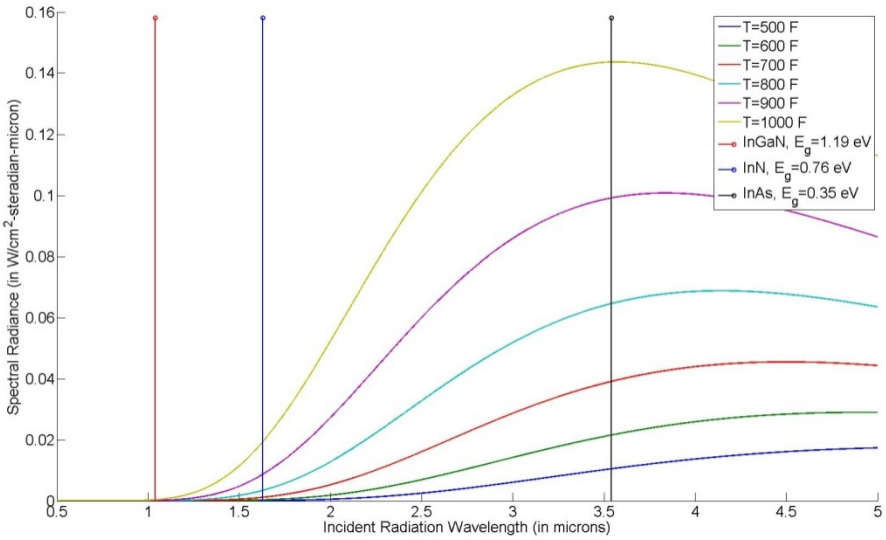

Figure 8. The spectral radiance of blackbodies at varying temperatures vs. their associated wavelengths.

The radiation spectrum received by each layer of the cell was not the same. MATLAB was used to extract information about how much of the incident radiation was absorbed by a given layer. This data was then subtracted from the incident radiation received by that layer to determine the amount of spectral intensity remaining after passing through the layer. This remaining spectral intensity was used as the incident radiation for the subsequent layer to account for absorption losses since the layers were not simulated together at the same time.

The model also does not account for any losses to the radiation intensity other than absorption by the TPV materials. The other major loss method that was not considered in this model is reflection of the incident radiation at any transitions between different materials.

The next chapter presents the results of this simulation and the author's interpretation of the meaning of these results.

THIS PAGE INTENTIONALLY LEFT BLANK

V. SIMULATION RESULTS

The focus of this thesis was to develop and test a multijunction TPV cell to determine the feasibility of using such a device as a supplemental electrical power source on board a nuclear submarine. The ATLAS output file recorded the output current for each layer of the cell at the applied anode voltage. These values are used to generate the I-V curve for a cell. The curves produced when the cell was exposed to the 500F blackbody spectrum are shown in Figure 9.

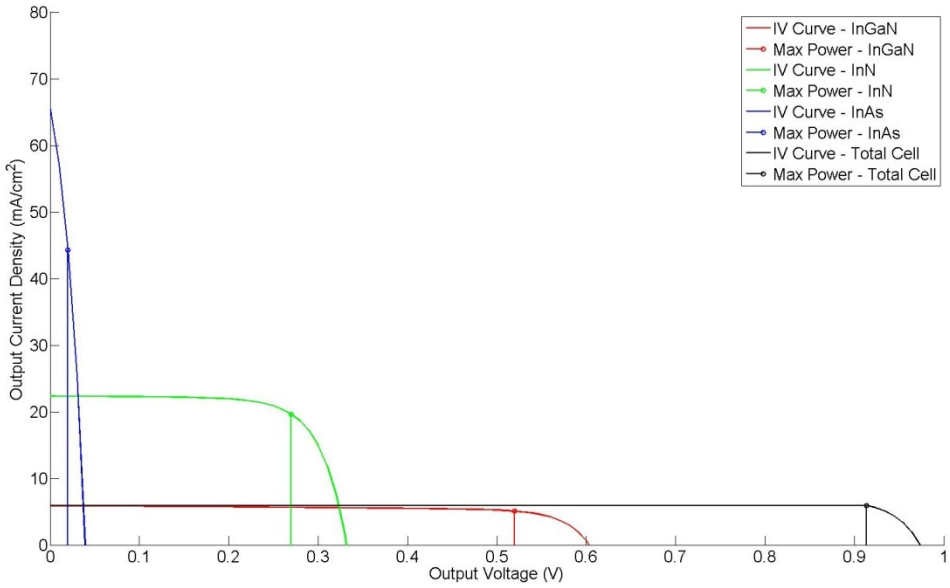

Figure 9. The I-V curves for each TPV layer and the combined cell when modeled using a 500F blackbody spectrum.

As described previously, these current and voltage values were used to determine the power output of the cell and, thus, its overall efficiency. The total cell output results are presented in Table 2. The average input power

was calculated by ATLAS based upon an integration of the spectral intensities for all wavelengths simulated in the input spectrum file.

Table 2. The comparison of TPV cell output at each blackbody radiation temperature.

Blackbody Temperature (F)	Maximum Current Density (mA/cm^2)	Maximum Voltage (V)	Maximum Output Power (mW/cm^2)	Average Input Power (mW/cm^2)	Cell Efficiency (%)
500	5.9008	0.9139	5.3925	28.7618	18.7489
600	11.1590	0.9699	10.8225	56.3377	19.2101
700	19.0251	0.9796	18.6372	100.1863	18.6026
800	28.7279	0.9847	28.2874	165.3810	17.1044
900	41.3669	1.0152	41.9953	257.4636	16.3112
1000	59.3913	1.0403	61.7859	376.8233	16.3965

As expected, the current density increases with blackbody temperature due to the rise of spectral intensity at each temperature. The author found two of the results to be particularly interesting.

First, the best performing version of the cell achieved an efficiency of 19.21%. Given that no optimization work was done for this cell, this level of efficiency points toward the viability of this device as a

supplemental power source. This level of conversion efficiency compared to the other temperatures indicates that the cell layer thicknesses and doping concentrations are the closest to the optimal values for the associated radiation spectrum at 600F.

Second, the author was pleased to note that at the given cell parameters, the 500F cell was the second most efficient. Again, this supports the viability of this system as a secondary power supply onboard a nuclear submarine. Optimizing the layer thicknesses and doping concentrations for this cell results in maximum output characteristics for the associated radiation spectrum.

The author's conclusions about the results of this work are presented in the final chapter of this thesis. The author also provides an explanation of areas in need of further research to enhance the capabilities of this model as well as some additional applications that could benefit from the use of this technology.

THIS PAGE INTENTIONALLY LEFT BLANK

VI. CONCLUSIONS AND RECOMMENDATIONS

A. CONCLUSIONS

The feasibility of using a multijunction TPV cell as a supplemental power source on a nuclear submarine was investigated in this thesis. A triple layer cell composed of InGaN, InN, and InAs was simulated in Silvaco's ATLAS TCAD program. The model was exposed to the IR radiation spectrum emitted by a blackbody source at temperatures of 500F to 1000F in 100F increments. The layers were simulated individually, and their electrical output was combined after the fact to determine the total electrical output of the cell as a whole.

The results of the simulation support the viability of this system as a supplemental power source for use with a nuclear reactor. The model demonstrated solid efficiency results even without optimization for the expected radiation spectrum. The model also showed that the system can be used effectively over a range of temperatures, thus allowing greater flexibility in the design of a future nuclear reactor that could take the greatest advantage of this system.

B. RECOMMENDATIONS

It has also shown that this is only the beginning of study for this particular model. There are several areas that need more focused development to further enhance the capabilities of this initial model. There are also more applications for this device beyond use on submarines that are worthy of further exploration.

1. Future Research Topics

There are several topics within this thesis that could provide additional benefits to the operation of the design model if they were the subject of further research work.

a. Cell Optimization

As highlighted earlier, this design has not undergone any optimization to its device parameters. Specifically, fine tuning the layer thicknesses and doping concentrations should result in improved current and voltage output and, thus, improved cell efficiency. MATLAB can be a powerful tool in optimizing ATLAS designs, as shown by Canfield [3] in his work to optimize TPV cells for higher cell operating temperatures.

Another area that could benefit from optimization would be matching the TPV cell resistance values at the expected input radiation spectrum. It can be seen in the data in Table 2 that the cell resistance value lowers as input spectral intensity rises. Specifically, the output voltage remains relatively constant while the output current increases by a factor of ten as the spectral intensity rises by a factor of 13. Matching the output resistance values could improve the efficiency for power transfer out of the cell.

b. Tunnel Junction Design

A common way of improving the performance of multijunction PV cells is the use of tunnel junctions to make a single monolithic device as opposed to having several separate layers. A tunnel junction is a very thin, highly-doped semiconductor layer that allows for easy flow

of electrons between photogenerating layers. The use of tunnel junctions also makes the final assembly of the complete cell easier by eliminating the need to design insulating materials to support the gap between layers.

c. Radiation Durability Study

An important topic that must be resolved to ensure the suitability of the design model for use with nuclear reactors is the durability of the design within gamma and neutron radiation fields. Lawrence Berkeley National Laboratory conducted a study [11] that demonstrated that InGaN can be exposed to high-energy charged particles at two to three orders of magnitude greater intensity that other semiconductor materials before it begins to experience deterioration of its electrical performance. Unfortunately, the author was unable to locate any studies related to the effect of high-energy gamma photons and neutrons on InGaN or any studies on the effects of any type of radiation on InN and InAs. An additional aspect of this study would be to determine if any of the materials used in this model undergo self-annealing at the system operating temperatures. If present, this self-annealing process could help to repair damage to the crystalline structure that would otherwise negatively impact the electrical output characteristics. These studies should help to determine the operating lifetime for this model when used with a nuclear reactor.

d. Material Properties Study

The accuracy of this model would be further enhanced by additional studies into the material properties

of InGaN and InN, specifically their optical properties. As noted in Section A.1 of Chapter IV, the author had to use optical index values that were approximations, estimations, or associated with other properties whose values are not consistent with the values actually used in the model. Further study into this area is needed to ensure that the model portrays the real-world operation of these materials to the best extent possible.

e. Advanced PV Materials

The author originally intended to develop PV materials that could also harness the energy found in the high-energy gamma photons and neutrons emitted due to the fission process. Due to time constraints, the author had to focus his efforts on developing an initial TPV model. The idea of capturing these other energy sources is still worthy of further work to develop and implement such materials.

f. Additional Converter Components

The author noted at the beginning of Chapter IV that this model does not consider the impact of the use of radiation emitters or filters on TPV cell output. Both of these devices could provide additional improvements to the output efficiency of the cell. The effects of these devices could be incorporated by alterations to the incident radiation beam used in the simulation. An emitter would help to focus the IR radation beam and increase the spectral intensity of the incident beam. A filter would preferentially allow the transmission of those photons whose energy levels matched the bandgaps of the materials

used in the model. Both of these devices are widely used in current TPV converters, and their effects should be included to improve the real-world accuracy of this model.

2. Additional Applications

The model developed in this thesis has applications beyond use in submarines. Other forms of nuclear power, both military and civilian, could benefit from the ability to utilize energy that is currently going to waste. This technology also holds great promise for inclusion on space craft needed for deep-space missions. Finally, this model could open a new field in the development of nuclear batteries.

a. Alternate Nuclear Power Sources

The model in this thesis could easily be adapted for use with other military and civilian nuclear reactors. Although power sources are not as difficult to come by on surface ships, this system could provide another backup power source for aircraft carriers. This design could also provide great benefit to the civilian nuclear power industry. The additional energy to be harnessed would provide a measureable increase to the total electrical power supplied by a given nuclear power plant.

b. Non-PV Space Craft

This system is also well suited for use in space craft that utilize radioisotope thermoelectric generators or nuclear reactors instead of traditional PV cells. The most commonly used systems for generating electricity from these two heat sources are only achieving efficiencies of

up to five percent [8]. Even without further optimization, the model presented in this thesis is achieving efficiencies of three to four times this amount.

c. Nuclear Batteries

Nuclear batteries were first developed in the 1960s and were similar in design to early RTGs. Newer versions have harnessed a group of materials called betavoltaics that undergo a process similar to the photoelectric effect except that they utilize beta particles emitted from radioactive isotopes. The author would like to recognize his wife, Rosemary Howard, as the originator of this next application. A new type of large-scale nuclear battery could be developed using materials that are designed to capture the gamma and neutron radiation being given off by spent reactor fuel cores. This would require developing materials that are able to generate electricity from these types of radiation but would be yet another way of harnessing energy that is currently considered to be without use. Given sufficient protective shielding and cooling support systems, this type of nuclear battery could provide a moderate amount of electrical power for use in remote locations.

APPENDIX A. ATLAS SOURCE CODE

This appendix contains the DeckBuild code used to simulate the TPV layers in ATLAS. Sections A, B, and C provide the code for each of the individual TPV layers.

A. INDIUM GALLIUM NITRIDE LAYER

```
go atlas

# LT John Howard
# Naval Postgraduate School
# June 2011

# This file describes the upper layer of a three-layer TPV
# cell. This cell is designed to have three
# thermophotovoltaic (TPV) layers to optimally absorb
# infrared radiation generated by the fission reaction in a
# nuclear reactor.
#
# Units used in the design of this cell are microns for
# length, atoms/cc for doping concentrations, and Kelvin
# for temperature, unless otherwise specified.

##### Constants

#### Output File Designations
### IV Curve Output
set IVName=TPV_500F_InGaN_IVCurve.log
### Cell Structure
set StructFile=TPV_500F_InGaN_Profile.str

#### Operating Temperature
set temperature=300

#### Cell Dimensions
### Baseline Number of Divisions/Layer
set divs=10

### Cell Width
set cellWidth=500
set zwidth=1e8/$cellWidth
set cellWidthHalf=$cellWidth/2
set cellWidthDiv1=$cellWidth/$divs
```

```
set cellWidthDiv2=$cellWidth/$divs/5
set cathodeWidthHalf=$cellWidthHalf*0.08

### Air Thickness
set airThick=0.5

### Upper TPV Layer
## Window Thickness
set windowThick=0.01
## Window Doping
set winDop=5e+017
## Emitter Thickness
set emitterThick=0.01
## Emitter Doping
set emitDop=5e+016
## Base Thickness
set baseThick=4
## Base Doping
set baseDop=1e+018
## BSF Thickness
set bsfThick=0.01
## BSF Doping
set bsfDop=5e19
## Layer Thickness
set layerThick=$windowThick+$emitterThick+$baseThick+\
     $bsfThick

### Conditional Dimensions
set bsfLo=$airThick+$layerThick
set bsfHi=$bsfLo-$bsfThick
set baseLo=$bsfHi
set baseHi=$baseLo-$baseThick
set emitterLo=$baseHi
set emitterHi=$emitterLo-$emitterThick
set windowLo=$emitterHi
set windowHi=$windowLo-$windowThick
set airLo=$windowHi
set airHi=$airLo-$airThick
set lightY=-5

##### Structure Specification

#### Mesh

mesh width=$zwidth auto
x.mesh loc=-$cellWidthHalf spac=$cellWidthDiv2
```

```
x.mesh loc=$cellWidthHalf spac=$cellWidthDiv2

#### Region

### Air
region num=1 material=Air x.min=-$cellWidthHalf \
     x.max=$cellWidthHalf y.min=$airHi y.max=$airLo

### Upper TPV Layer
## Window
region num=2 material=InGaN x.min=-$cellWidthHalf \
     x.max=$cellWidthHalf y.min=$windowHi y.max=$windowLo
## Emitter
region num=3 material=InGaN x.min=-$cellWidthHalf \
     x.max=$cellWidthHalf y.min=$emitterHi y.max=$emitterLo
## Base
region num=4 material=InGaN x.min=-$cellWidthHalf \
     x.max=$cellWidthHalf y.min=$baseHi y.max=$baseLo
## BSF
region num=5 material=InGaN x.min=-$cellWidthHalf \
     x.max=$cellWidthHalf y.min=$bsfHi y.max=$bsfLo

#### Electrodes

### Upper TPV Layer
electrode name=cathode material=Gold x.min= \
    -$cathodeWidthHalf x.max=$cathodeWidthHalf \
    y.min=$windowHi-0.1 y.max=$windowHi
electrode name=anode material=Gold x.min=-$cellWidthHalf \
     x.max=$cellWidthHalf y.min=$bsfLo y.max=$bsfLo

#### Doping - n-type emitter on p-type base

### Upper TPV Layer
## Window
doping uniform region=2 n.type conc=$winDop
## Emitter
doping uniform region=3 n.type conc=$emitDop
## Base
doping uniform region=4 p.type conc=$baseDop
## BSF
doping uniform region=5 p.type conc=$bsfDop

##### Material Models Specification

#### Material
```

```
### Air
material material=Air real.index=3.3 imag.index=0

### InGaN
## Upper TPV Layer
material material=InGaN EG300=1.19 real.index=1.52 \
    imag.index=1.68
# real.index is an approximation, imag.index is an estimate

### Gold
material material=Gold real.index=1.2 imag.index=1.8

#### Models
models srh bgn temp=$temperature print

##### Light Beam Specification

#### Infrared Radiation
beam num=1 x.origin=0 y.origin=$lightY angle=90 \
    power.file=BBRad500F.spec wavel.num=2251 back.refl

##### Numerical Method Selection
method gummel newton maxtraps=10 itlimit=100 climit=1\
    dvmax=0.1

##### Solution Specification

#### Solve

solve initial
solve b1=1.0

output opt.int
save outfile=$StructFile

log outfile=$IVName

solve vanode=0.0 name=anode vstep=0.01 vfinal=1

quit
```

B. INDIUM NITRIDE LAYER

```
go atlas

# LT John Howard
# Naval Postgraduate School
# June 2011

# This file describes the middle layer of a three-layer TPV
# cell. This cell is designed to have three
# thermophotovoltaic (TPV) layers to optimally absorb
# infrared radiation generated by the fission reaction in a
# nuclear reactor.
#
# Units used in the design of this cell are microns for
# length, atoms/cc for doping concentrations, and Kelvin
# for temperature, unless otherwise specified.

##### Constants

#### Output File Designations
### IV Curve Output
set IVName=TPV_500F_InN_IVCurve.log
### Cell Structure
set StructFile=TPV_500F_InN_Profile.str

#### Operating Temperature
set temperature=300

#### Cell Dimensions
### Baseline Number of Divisions/Layer
set divs=10

### Cell Width
set cellWidth=500
set zwidth=1e8/$cellWidth
set cellWidthHalf=$cellWidth/2
set cellWidthDiv1=$cellWidth/$divs
set cellWidthDiv2=$cellWidth/$divs/5
set cathodeWidthHalf=$cellWidthHalf*0.08

### Air Thickness
set airThick=0.5

### Middle TPV Layer
## Window Thickness
```

```
set windowThick=0.01
## Window Doping
set winDop=5e+017
## Emitter Thickness
set emitterThick=0.05
## Emitter Doping
set emitDop=5e+016
## Base Thickness
set baseThick=10
## Base Doping
set baseDop=1e+018
## BSF Thickness
set bsfThick=0.01
## BSF Doping
set bsfDop=5e19
## Layer Thickness
set layerThick=$windowThick+$emitterThick+$baseThick+ \
    $bsfThick

### Conditional Dimensions
set bsfLo=$airThick+$layerThick
set bsfHi=$bsfLo-$bsfThick
set baseLo=$bsfHi
set baseHi=$baseLo-$baseThick
set emitterLo=$baseHi
set emitterHi=$emitterLo-$emitterThick
set windowLo=$emitterHi
set windowHi=$windowLo-$windowThick
set airLo=$windowHi
set airHi=$airLo-$airThick
set lightY=-5

##### Structure Specification

#### Mesh

mesh width=$zwidth auto
x.mesh loc=-$cellWidthHalf spac=$cellWidthDiv2
x.mesh loc=$cellWidthHalf spac=$cellWidthDiv2

#### Region

### Air
region num=1 material=Air x.min=-$cellWidthHalf \
    x.max=$cellWidthHalf y.min=$airHi y.max=$airLo
```

```
### Middle TPV Layer
## Window
region num=2 material=InN x.min=-$cellWidthHalf \
    x.max=$cellWidthHalf y.min=$windowHi y.max=$windowLo
## Emitter
region num=3 material=InN x.min=-$cellWidthHalf \
    x.max=$cellWidthHalf y.min=$emitterHi y.max=$emitterLo
## Base
region num=4 material=InN x.min=-$cellWidthHalf \
    x.max=$cellWidthHalf y.min=$baseHi y.max=$baseLo
## BSF
region num=5 material=InN x.min=-$cellWidthHalf \
    x.max=$cellWidthHalf y.min=$bsfHi y.max=$bsfLo

#### Electrodes

### Middle TPV Layer
electrode name=cathode material=Gold x.min= \
    -$cathodeWidthHalf x.max=$cathodeWidthHalf \
    y.min=$windowHi-0.1 y.max=$windowHi
electrode name=anode material=Gold x.min=-$cellWidthHalf \
     x.max=$cellWidthHalf y.min=$bsfLo y.max=$bsfLo

#### Doping - n-type emitter on p-type base

### Middle TPV Layer
## Window
doping uniform region=2 n.type conc=$winDop
## Emitter
doping uniform region=3 n.type conc=$emitDop
## Base
doping uniform region=4 p.type conc=$baseDop
## BSF
doping uniform region=5 p.type conc=$bsfDop

##### Material Models Specification

#### Material
### Air
material material=Air real.index=3.3 imag.index=0

### InN
## Middle TPV Layer
material material=InN EG300=0.76 real.index=2.71 \
    imag.index=0.54
```

```
### Gold
material material=Gold real.index=1.2 imag.index=1.8

#### Models
models srh bgn temp=$temperature print

##### Light Beam Specification

#### Infrared Radiation
beam num=1 x.origin=0 y.origin=$lightY angle=90 \
    power.file=Post_InGaN_500F.spec wavel.num=2251 \
    back.refl

##### Numerical Method Selection

method gummel newton maxtraps=10 itlimit=100 climit=1 \
    dvmax=0.1

##### Solution Specification

### Solve

solve initial
solve b1=1.0

output opt.int
save outfile=$StructFile

log outfile=$IVName

solve vanode=0.0 name=anode vstep=0.01 vfinal=1

quit
```

C. INDIUM ARSENIDE LAYER

```
go atlas

# LT John Howard
# Naval Postgraduate School
# June 2011

# This file describes the lower layer of a three-layer TPV
# cell. This cell is designed to have three
# thermophotovoltaic (TPV) layers to optimally absorb
# infrared radiation generated by the fission reaction in a
```

```
# nuclear reactor.
#
# Units used in the design of this cell are microns for
# length, atoms/cc for doping concentrations, and Kelvin
# for temperature, unless otherwise specified.

##### Constants

#### Output File Designations
### IV Curve Output
set IVName=TPV_500F_InAs_IVCurve.log
### Cell Structure
set StructFile=TPV_500F_InAs_Profile.str

#### Operating Temperature
set temperature=300

#### Cell Dimensions
### Baseline Number of Divisions/Layer
set divs=10

### Cell Width
set cellWidth=500
set zwidth=1e8/$cellWidth
set cellWidthHalf=$cellWidth/2
set cellWidthDiv1=$cellWidth/$divs
set cellWidthDiv2=$cellWidth/$divs/5
set cathodeWidthHalf=$cellWidthHalf*0.08

### Air Thickness
set airThick=0.5

### Lower TPV Layer
## Window Thickness
set windowThick=0.05
## Window Doping
set winDop=7e+018
## Emitter Thickness
set emitterThick=0.1
## Emitter Doping
set emitDop=3e+018
## Base Thickness
set baseThick=5
## Base doping
set baseDop=2e+019
## BSF Thickness
```

```
set bsfThick=0.01
## BSF Doping
set bsfDop=5e19
## Layer Thickness
set layerThick=$windowThick+$emitterThick+$baseThick+ \
    $bsfThick

### Conditional Dimensions
set bsfLo=$airThick+$layerThick
set bsfHi=$bsfLo-$bsfThick
set baseLo=$bsfHi
set baseHi=$baseLo-$baseThick
set emitterLo=$baseHi
set emitterHi=$emitterLo-$emitterThick
set windowLo=$emitterHi
set windowHi=$windowLo-$windowThick
set airLo=$windowHi
set airHi=$airLo-$airThick
set lightY=-5

##### Structure Specification

#### Mesh

mesh width=$zwidth auto
x.mesh loc=-$cellWidthHalf spac=$cellWidthDiv2
x.mesh loc=$cellWidthHalf spac=$cellWidthDiv2

#### Region

### Air
region num=1 material=Air x.min=-$cellWidthHalf \
    x.max=$cellWidthHalf y.min=$airHi y.max=$airLo

### Lower TPV Layer
## Window
region num=2 material=InAs x.min=-$cellWidthHalf \
    x.max=$cellWidthHalf y.min=$windowHi y.max=$windowLo
## Emitter
region num=3 material=InAs x.min=-$cellWidthHalf \
    x.max=$cellWidthHalf y.min=$emitterHi y.max=$emitterLo
## Base
region num=4 material=InAs x.min=-$cellWidthHalf \
    x.max=$cellWidthHalf y.min=$baseHi y.max=$baseLo
## BSF
region num=5 material=InAs x.min=-$cellWidthHalf \
```

```
    x.max=$cellWidthHalf y.min=$bsfHi y.max=$bsfLo

#### Electrodes

### Lower TPV Layer
electrode name=cathode material=Gold x.min= \
    -$cathodeWidthHalf x.max=$cathodeWidthHalf \
    y.min=$windowHi-0.1 y.max=$windowHi
electrode  name=anode  material=Gold  x.min=-$cellWidthHalf  \
     x.max=$cellWidthHalf y.min=$bsfLo y.max=$bsfLo

#### Doping - n-type emitter on p-type base

### Lower TPV Layer
## Window
doping uniform region=2 n.type conc=$winDop
## Emitter
doping uniform region=3 n.type conc=$emitDop
## Base
doping uniform region=4 p.type conc=$baseDop
## BSF
doping uniform region=5 p.type conc=$bsfDop

##### Material Models Specification

#### Material
### Air
material material=Air real.index=3.3 imag.index=0

### InAs
## Lower TPV Layer
material material=InAs sopra=inas.nk

### Gold
material material=Gold real.index=1.2 imag.index=1.8

#### Models
models srh bgn temp=$temperature print

##### Light Beam Specification

#### Infrared Radiation
beam num=1 x.origin=0 y.origin=$lightY angle=90 \
    power.file=Post_InN_500F.spec wavel.num=2251 back.refl

##### Numerical Method Selection
```

```
method gummel newton maxtraps=10 itlimit=100 climit=1 \
    dvmax=0.1

##### Solution Specification

#### Solve

solve initial
solve b1=1.0

output opt.int
struct outfile=$StructFile

log outfile=$IVName

solve vanode=0.0 name=anode vstep=0.01 vfinal=1

quit
```

APPENDIX B. MATLAB SOURCE CODE

This appendix contains the MATLAB script and function files used to extract and process the TPV cell performance data. Some of the script files are specific to the temperature of the simulation and so only one example of those files is included here.

A. DATA PROCESSOR

This set of files is used to extract the data needed to calculate the cell operating parameters and generate the current-voltage curves for the complete cell at the given temperature.

1. Script File for 500F

The script file (DataProcessor_500F.m) supplies the file names for the data to be extracted and processed. This data is printed to the MATLAB command window (similar to the DeckBuild run-time output), plotted in terms of voltage vs. current, and exported to an Excel spreadsheet to allow for comparison of the combined cell results at each temperature.

```
% Reads data from a Silvaco *.log file and generates the IV
% Curves for the associated TPV cells.
%
% LT John Howard
% Naval Postgraduate School, Monterey, CA
% April 30, 2011

clf
clear
clc

% Establish initial parameters
Cell_Current_Out=1e6;
```

```
Cell_Voltage_Out=0;
Cell_Optical_Intensity=0;
layers=0;

% Process data from Upper TPV Layer
[Cell_Current_Out,Cell_Voltage_Out,...
    Cell_Optical_Intensity,Voc_slope]=...
    DataProcFunc('TPV_500F_InGaN_IVCurve.log','-r',...
    Cell_Current_Out,Cell_Voltage_Out,...
    Cell_Optical_Intensity);
layers=layers+1;
Voc_slope_total=Voc_slope;
fprintf('----------\n\n')

% Process data from Middle TPV Layer
[Cell_Current_Out,Cell_Voltage_Out,...
    Cell_Optical_Intensity,Voc_slope]=...
    DataProcFunc('TPV_500F_InN_IVCurve.log','-g',...
    Cell_Current_Out,Cell_Voltage_Out,...
    Cell_Optical_Intensity);
layers=layers+1;
fprintf('----------\n\n')

% Process data from Lower TPV Layer
[Cell_Current_Out,Cell_Voltage_Out,...
    Cell_Optical_Intensity,Voc_slope]=...
    DataProcFunc('TPV_500F_InAs_IVCurve.log','-b',...
    Cell_Current_Out,Cell_Voltage_Out,...
    Cell_Optical_Intensity);
layers=layers+1;
fprintf('----------\n\n')

% Process data for Total Cell
for i=size(Voc_slope_total,1)+1:-1:2
    V_total(i)=Cell_Voltage_Out-(size(Voc_slope_total,1)...
        +1-i)*0.01;
end

I_total=zeros(1,size(V_total,2));
V_delta=0.01;

for i=size(Voc_slope_total,1):-1:1

I_total(i)=I_total(i+1)+V_delta*abs(Voc_slope_total(i));
    if I_total(i)*1000>Cell_Current_Out
        I_total(i)=Cell_Current_Out/1000;
```

```
    end
end

I_total=I_total*1000;

P_total=I_total.*V_total;

[Pmax_total,Pmax_total_ind]=max(P_total);

Vmax_total=V_total(Pmax_total_ind);

Imax_total=I_total(Pmax_total_ind);

FF_total=Pmax_total/(Cell_Current_Out*Cell_Voltage_Out)...
    *100;

Cell_Optical_Intensity=Cell_Optical_Intensity*1e3/layers;

Cell_Efficiency=Pmax_total/Cell_Optical_Intensity*100;

fprintf('Total Cell Data\n\n')
fprintf('Short Circuit current (mA/cm^2): %f\n\n',...
    Cell_Current_Out)
fprintf('Open Circuit voltage (V): %f\n\n',...
    Cell_Voltage_Out)
fprintf('Maximum Power (mW/cm^2): %f\n\n',Pmax_total)
fprintf('Maximum Voltage (V): %f\n\n',Vmax_total)
fprintf('Maximum Current (mA/cm^2): %f\n\n',Imax_total)
fprintf('Fill Factor (%%): %f\n\n',FF_total)
fprintf('Optical Intensity (mW/cm^2): %f\n\n',...
    Cell_Optical_Intensity)
fprintf('Cell Efficiency (%%): %f\n\n',Cell_Efficiency)

%Plot Total Cell data and modify output figure
plot(V_total,I_total,'-k','linewidth',2)
stem(Vmax_total,Imax_total,'-k','linewidth',2)
legend('IV Curve - InGaN','Max Power - InGaN',...
    'IV Curve - InN','Max Power - InN',...
    'IV Curve - InAs','Max Power - InAs',...
    'IV Curve - Total Cell','Max Power - Total Cell')
axis([0 1 0 80])
xlabel('Output Voltage (V)','fontsize',20)
ylabel('Output Current Density (mA/cm^2)','fontsize',20)
set(gca,'fontsize',20)

% Output Combined IV Curve Data to Spreadsheet for
```

```
% comparison
Total_500F_Data=[V_total' I_total'];
xlswrite('CombinedCellData.xls',Total_500F_Data,...
    'Total-500F')
```

2. Data Processor Function File

This function file (DatProcFunc.m) performs the data extraction from the specified ATLAS log file and returns the specified parameters.

```
function [Cell_Current_Out,Cell_Voltage_Out,...
    Cell_Optical_Intensity,Voc_slope]=DataProcFunc(...
    Data_File,Plot_Spec,Cell_Current_Out,...
    Cell_Voltage_Out,Cell_Optical_Intensity)
%DATAPROCFUNC Extracts photovoltaic cell performance data
%from the given Silvaco log file.
%   This function extracts values of anode voltage and
%   cathode current from standardized Silvaco ATLAS log
%   files.  This data is then used to calculate the
%   performance values for the given cell, displays these
%   results to the Command Window, and generates a plot of
%   the associated I-V Curve and point of maximum power
%   output.
%
%   LT John Howard
%   Naval Postgraduate School, Monterey, CA
%   May 12, 2011

Data_scale=1000;    % Converts from A/cm^2 to mA/cm^2

Data=dlmread(Data_File,' ',20,1);

Isc_sort=max(Data);
Isc=Isc_sort(11)*Data_scale;

n_search=0;

for i=1:size(Data,1)
    if Data(i,11)<0
        n_search=i;
        break;
    end
    n_search=i;
end
```

```
Voc_slope=zeros(n_search-1,1);

for i=2:n_search
    Voc_slope(i-1,1)=(Data(i,11)-Data(i-1,11))/...
        (Data(i,12)-Data(i-1,12));
end

Voc=Data(n_search-1,12)-Data(n_search-1,11)/...
    Voc_slope(end,1);

Power=Data(1:n_search,11).*Data_scale.*Data(1:n_search,12);

[Pmax,Pmax_ind]=max(Power);

Vmax=Data(Pmax_ind,12);

Imax=Data(Pmax_ind,11)*Data_scale;

FF=Pmax/(Isc*Voc)*100;

Opt_Int=sum(Data(1:n_search,1))/n_search;

Eff=Pmax/(Opt_Int*1e3)*100;

figure(1)
hold on
plot(Data(1:n_search,12),Data(1:n_search,11).*...
    Data_scale,Plot_Spec,'linewidth',2)
stem(Vmax,Imax,Plot_Spec,'linewidth',2)

fprintf('Source Data File: %s\n\n',Data_File)
fprintf('Short Circuit current (mA/cm^2): %f\n\n',Isc)
fprintf('Open Circuit voltage (V): %f\n\n',Voc)
fprintf('Maximum Power (mW/cm^2): %f\n\n',Pmax)
fprintf('Maximum Voltage (V): %f\n\n',Vmax)
fprintf('Maximum Current (mA/cm^2): %f\n\n',Imax)
fprintf('Fill Factor (%%): %f\n\n',FF)
fprintf('Optical Intensity (W/cm^2): %f\n\n',Opt_Int)
fprintf('Cell Efficiency (%%): %f\n\n',Eff)

if Isc<Cell_Current_Out
    Cell_Current_Out=Isc;
end
Cell_Voltage_Out=Cell_Voltage_Out+Voc;
```

```
Cell_Optical_Intensity=Cell_Optical_Intensity+Opt_Int;
end
```

B. ATLAS SPECTRUM FILE CALCULATOR

This set of files is used to create the radiation spectrum input files for ATLAS. The file in the first section uses the blackbody radiation equation to generate the initial spectrum used with the upper TPV layer. The next two sections have the files used to generate the spectrum file downstream of the given layer. This allows ATLAS to properly simulate the middle and lower layers by accounting for the radiation that was absorbed in the previous layer.

1. Blackbody Radiation Calculator

This file (BlackbodyRadCalc.m) generates the original blackbody radiation spectrum for each of the six blackbody temperatures used in this model and creates the associated ATLAS spectrum files.

```
% LT John Howard
% Naval Postgraduate School, Monterey, CA
% January 31, 2011

% This program calculates the blackbody radiation spectrum
% based on a given heat source temperature, plots the
% spectral intensity vs. wavelength, and exports the
% spectral intensity into data files to be read by ATLAS.

clf
clear
clc

% Constants
c=2.998e8;      % Speed of light in a vacuum, in meters per
                % second
h=6.626e-34;    % Planck's Constant, in Joule-seconds
k=1.381e-23;    % Boltzmann's Constant, in Joules per
                % Kelvin
```

```
% Variables to be considered
T_F=500:100:1000;   % Temperature of blackbody source, in
                    % degrees Fahrenheit
lambda=0.5:0.002:5; % Wavelength of radiation, in microns

% Calculations
T_K=5/9.*(T_F-32)+273;  % Temperature of blackbody source,
                        % in Kelvin

Spec_Rad=zeros(size(T_K,2),size(lambda,2));
        % Preallocates Spectral Radiance vector

for i=1:size(T_K,2)
    Spec_Rad(i,:)=2e24*h*c^2./lambda.^5./(exp(1e6*h*c./...
        (lambda*k.*T_K(i)))-1)/1e4;
        % Spectral Radiance in W cm^-2 sr^-1 um^-1
end

% Plot Spectral Radiance versus Wavelength
figure(1)
hold on
plot(lambda,Spec_Rad,'linewidth',2)
set(gca,'fontsize',20)
stem(1.04,1.1*max(max(Spec_Rad)),'-r','linewidth',2)
stem(1.63,1.1*max(max(Spec_Rad)),'-b','linewidth',2)
stem(3.54,1.1*max(max(Spec_Rad)),'-k','linewidth',2)
xlabel('Incident Radiation Wavelength (in microns)',...
    'fontsize',20)
ylabel('Spectral Radiance (in W/cm^2-steradian-micron)'...
    ,'fontsize',20)
legend('T=500 F','T=600 F','T=700 F','T=800 F',...
    'T=900 F','T=1000 F','InGaN, E_g=1.19 eV',...
    'InN, E_g=0.76 eV','InAs, E_g=0.35 eV','Location',...
    'Northeast')

% Export Spectral Radiance Data for use in DeckBuild
Spec_Rad_500=[lambda;Spec_Rad(1,:)];
Spec_Rad_600=[lambda;Spec_Rad(2,:)];
Spec_Rad_700=[lambda;Spec_Rad(3,:)];
Spec_Rad_800=[lambda;Spec_Rad(4,:)];
Spec_Rad_900=[lambda;Spec_Rad(5,:)];
Spec_Rad_1000=[lambda;Spec_Rad(6,:)];

fid=fopen('BBRad500K.spec','wt');
fprintf(fid,'# Blackbody Radiation Spectrum for 500 F\n');
```

```
fprintf(fid,'%0.0f\n',size(Spec_Rad_500,2));
fprintf(fid,'%6.3f %15.12f\n',Spec_Rad_500);
fclose(fid);

fid=fopen('BBRad600K.spec','wt');
fprintf(fid,'# Blackbody Radiation Spectrum for 600 F\n');
fprintf(fid,'%0.0f\n',size(Spec_Rad_600,2));
fprintf(fid,'%.3f %15.12f\n',Spec_Rad_600);
fclose(fid);

fid=fopen('BBRad700K.spec','wt');
fprintf(fid,'# Blackbody Radiation Spectrum for 700 F\n');
fprintf(fid,'%0.0f\n',size(Spec_Rad_700,2));
fprintf(fid,'%.3f %15.12f\n',Spec_Rad_700);
fclose(fid);

fid=fopen('BBRad800K.spec','wt');
fprintf(fid,'# Blackbody Radiation Spectrum for 800 F\n');
fprintf(fid,'%0.0f\n',size(Spec_Rad_800,2));
fprintf(fid,'%.3f %15.12f\n',Spec_Rad_800);
fclose(fid);

fid=fopen('BBRad900K.spec','wt');
fprintf(fid,'# Blackbody Radiation Spectrum for 900 F\n');
fprintf(fid,'%0.0f\n',size(Spec_Rad_900,2));
fprintf(fid,'%.3f %15.12f\n',Spec_Rad_900);
fclose(fid);

fid=fopen('BBRad1000K.spec','wt');
fprintf(fid,'# Blackbody Radiation Spectrum for 1000 F\n');
fprintf(fid,'%0.0f\n',size(Spec_Rad_1000,2));
fprintf(fid,'%.3f %15.12f\n',Spec_Rad_1000);
fclose(fid);
```

2. Post-layer Radiation Spectrum Calculator

This file (Post_Layer_Rad_Spec_500F.m) generates the radiation spectrum file for the remaining spectral intensity after passing through the given input layer at the particular blackbody temperature.

```
% Generate new optical spectrum file after passing through
% the given layer.
%
% LT John Howard
```

```
% Naval Postgraduate School, Monterey, CA
% May 13, 2011

clear
clc

Type=input('Enter 1 for Post-InGaN or 2 for Post-InN: ');

if Type==1
    Spec_Data=RadSpecProcFunc(...
        'TPV_500F_InGaN_Profile.str','Post_InGaN',...
        'BBRad500F.spec',0,878,1373);
    fid=fopen('Post_InGaN_500K.spec','w+');
    fprintf(fid,...
        '# Post-InGaN Radiation Spectrum for 500 F\n');
    fprintf(fid,'%.0f\n',size(Spec_Data,2));
    fprintf(fid,'%.3f %15.12f\n',Spec_Data);
    fclose(fid);
    fprintf('\nDone with post-InGan file.\n\n')
end

if Type==2
    Spec_Data=RadSpecProcFunc(...
        'TPV_500F_InN_Profile.str','Post_InN',...
        'Post_InGaN_500K.spec',1,656,1594);
    fid=fopen('Post_InN_500F.spec','w+');
    fprintf(fid,...
        '# Post-InN Radiation Spectrum for 500 F\n');
    fprintf(fid,'%.0f\n',size(Spec_Data,2));
    fprintf(fid,'%.3f %15.12f\n',Spec_Data);
    fclose(fid);
    fprintf('\nDone with post-InN file.\n\n')
end
```

3. Radiation Spectrum Process Function File

This file is used by each of the temperature specific post-layer radiation spectrum calculator files. The parameters of Block_15_Cells, Block_16_Cells, and Block_19_Cells refer to the number of wavelengths in the SpectralData.xls file that have data in 15, 16, or 19 row blocks. These numbers must be manually determined by reviewing the Excel spreadsheet after the process has been

run the first time at a given temperature. The author noted that the post-InGaN spectrum data had only 16 and 19 block sections, while the post-InN spectrum data started with one 15 block section and the rest of the data was in 16 and 19 block sections. Once the correct ratio of sections has been determined, the process needs to be run again using those correct numbers to ensure that the resulting spectrum file contains all the expected wavelengths and spectral intensities.

```
function [Spec_Data]=RadSpecProcFunc(Data_File,...
    Sheet_Name,Orig_File,Block_15_Cells,Block_16_Cells,...
    Block_19_Cells)
%RADSPECPROCFUNC Generates new post-layer optical spectrum
%   file.
%   This function extracts values of optical intensity at
%   varying wavelengths from standardized Silvaco ATLAS
%   structure files.  This data is then used to generate
%   a new optical spectrum file for use with the subsequent
%   layer.
%
%   LT John Howard
%   Naval Postgraduate School, Monterey, CA
%   May 12, 2011

% Extracts layer absorption data from the given ATLAS
% structure file
fid1=fopen(Data_File,'r');
Spec_Data_Raw=fscanf(fid1,'%c');
fclose(fid1);

% Extracts spectral intensity data from pre-layer spectrum
% file
Spec_Data_Mod0=dlmread(Orig_File,' ',2,1);
Spec_Data_Size=dlmread(Orig_File,' ',[1 0 1 0]);
index=strfind(Spec_Data_Raw,'R');

% Transfers data to a text file for processing into MATLAB
Spec_Data_Mod1=Spec_Data_Raw(index(4):end);
fid2=fopen('TempData.txt','w');
fwrite(fid2,Spec_Data_Mod1);
fclose(fid2);
Spec_Data_Mod2=dlmread('TempData.txt',' ',0,1);
```

```
Spec_Data_Mod3=Spec_Data_Mod2(:,4:5);
delete('TempData.txt');

% Generates Excel spreadsheet with spectral absorption data
% the layer being processed
xlswrite('SpectralData.xls',Spec_Data_Mod3,Sheet_Name)

% Initializes matrices based on expected number of data
% points
Spec_Data_Mod4a=zeros(Block_16_Cells,2);
Spec_Data_Mod4b=zeros(Block_19_Cells,2);
Spec_Data_Mod5=zeros(Spec_Data_Size,2);

% Generates the post-layer spectral intensity values
if Block_15_Cells==0
    for i=1:Block_16_Cells
        Spec_Data_Mod4a(i,1)=mean(Spec_Data_Mod3(...
            (i*16-15):(i*16),1),1);
        Spec_Data_Mod4a(i,2)=mean(Spec_Data_Mod3(...
            (i*16-15):(i*16),2),1);
    end

    for i=1:Block_19_Cells
        index=Block_16_Cells*16+i*19-18;
        Spec_Data_Mod4b(i,1)=mean(Spec_Data_Mod3(...
            (index):(index+18),1),1);
        Spec_Data_Mod4b(i,2)=mean(Spec_Data_Mod3(...
            (index):(index+18),2),1);
    end

    for i=1:Block_16_Cells
        Spec_Data_Mod5(i,:)=[Spec_Data_Mod4a(i,1) ...
            (Spec_Data_Mod0(i,2)-Spec_Data_Mod4a(i,2))];
    end

    for i=1:Block_19_Cells
        Spec_Data_Mod5(i+Block_16_Cells,:)=[...
            Spec_Data_Mod4b(i,1) (Spec_Data_Mod0(i+...
            Block_16_Cells,2)-Spec_Data_Mod4b(i,2))];
        Spec_Data=Spec_Data_Mod5';
    end
else
    Spec_Data_Mod4c(1,1)=mean(Spec_Data_Mod3(1:15,1),1);
    Spec_Data_Mod4c(1,2)=mean(Spec_Data_Mod3(1:15,2),1);

    for i=1:Block_16_Cells
```

```
        Spec_Data_Mod4a(i,1)=mean(Spec_Data_Mod3((i*16):...
            (i*16+15),1),1);
        Spec_Data_Mod4a(i,2)=mean(Spec_Data_Mod3((i*16):...
            (i*16+15),2),1);
    end

    for i=1:Block_19_Cells
        index=Block_16_Cells*16+i*19-3;
        Spec_Data_Mod4b(i,1)=mean(Spec_Data_Mod3(index:...
            (index+18),1),1);
        Spec_Data_Mod4b(i,2)=mean(Spec_Data_Mod3(index:...
            (index+18),2),1);
    end

    Spec_Data_Mod5=Spec_Data_Mod4c;

    for i=1:Block_16_Cells
        Spec_Data_Mod5(i+1,:)=[Spec_Data_Mod4a(i,1) ...
            (Spec_Data_Mod0(i,2)-Spec_Data_Mod4a(i,2))];
    end

    for i=1:Block_19_Cells
        Spec_Data_Mod5(i+1+Block_16_Cells,:)=[...
            Spec_Data_Mod4b(i,1) (Spec_Data_Mod0(i+...
            Block_16_Cells,2)-Spec_Data_Mod4b(i,2))];
        Spec_Data=Spec_Data_Mod5';
    end
end
```

C. MISCELLANEOUS SUPPORT FILES

This section contains the remaining MATLAB scripts that were used to generate this thesis.

1. Indium Gallium Nitride Bandgap Calculator

This file determines the ICF required to achieve the desired E_g for InGaN. It also plots the curve of ICF vs. E_g and shows the ICF for the desired InGaN E_g and the ICF equivalent to the uppermost frequency of the IR spectrum.

```
% Determines the required Indium Concentration Fraction
% (ICF) for achieving an Indium Gallium Nitride (InGaN)
% bandgap energy (Eg) of 1.19eV and plots the ICF vs. Eg
```

```
% graph.
%
% LT John Howard
% Naval Postgraduate School, Monterey, CA
% October 26, 2010

clf
clear
clc

% Constants (bandgaps given in eV)
Eg_InN=0.76;    % Eg for Indium Nitride
Eg_GaN=3.42;    % Eg for Gallium Nitride
b=1.44;         % InGaN Eg Bowing Parameter

% Determine Eg Range based on ICF "x"
x=0:0.001:1;
Eg_InGaN=((1-x).*Eg_GaN)+(x.*Eg_InN)-(b.*x.*(1-x));

% Plot InGaN Eg vs. ICF "x"
plot(x,Eg_InGaN,'-k','linewidth',2)
xlabel('Indium Concentration Fraction ''x''','fontsize',20)
ylabel('Indium Gallium Nitride Bandgap (eV)','fontsize',20)
set(gca,'fontsize',20)

% Determines required ICF values based upon desired Eg
% values
x_InGaN_layer=x(1.189<Eg_InGaN&Eg_InGaN<1.191)
Eg_InGaN_layer=Eg_InGaN(1.189<Eg_InGaN&Eg_InGaN<1.191)

% Determines ICF equivalent for maximum infrared frequency
x_IR_upper=x(1.589<Eg_InGaN&Eg_InGaN<1.591)
Eg_IR_upper=Eg_InGaN(1.589<Eg_InGaN&Eg_InGaN<1.591)

% Plot Selected Eg vs. ICF "x"
hold on
stem(x_InGaN_layer,Eg_InGaN_layer,'-b','linewidth',2)
stem(x_IR_upper,Eg_IR_upper,'-r','linewidth',2)
legend('E_g vs. x','InGaN Layer (E_g=1.19, x=0.73)',...
    'Upper Bound of IR (E_g=1.59)')
```

2. Photon Energy to Wavelength Calculator

This file was written by Michalopoulos [1] to convert photon energy in electron volts into its equivalent wavelength in microns.

```
function [um] = ev2um(ev)
% EV2UM Converts photon energy (eV) into wavelength (um).
% (c)2001 by P. Michalopoulos

h = 6.6260755e-34;
eV = 1.60218e-19;
c = 2.99792458e8;
ev = ev * eV;
f = ev / h;
wavel = c ./ f;
um = wavel / 1e-6;

end
```

3. Wavelength to Photon Energy Calculator

This file was written by Michalopoulos [1] to convert photon wavelength in microns into its equivalent energy in electron volts.

```
function ev = um2ev(um)
% UM2EV Converts photon wavelength (um) into energy (eV).
% (c)2001 by P. Michalopoulos

h = 6.6260755e-34;
eV = 1.60218e-19;
c = 2.99792458e8;
wavel = um * 1e-6;
f = c ./ wavel;
ev = h * f;
ev = ev ./ eV;

end
```

LIST OF REFERENCES

[1] P. Michalopoulos, “A novel approach for the development and optimization of state-of-the-art photovoltaic devices using Silvaco,” M.S. thesis, Naval Postgraduate School, Monterey, CA, 2002.

[2] M. Green, “The verification of Silvaco as a solar cell simulation tool and the design and optimization of a four-junction solar cell,” M.S. thesis, Naval Postgraduate School, Monterey, CA, 2002.

[3] B. Canfield, “Advanced modeling of high temperature performance of indium gallium arsenide thermophotovoltaic cells,” M.S. thesis, Naval Postgraduate School, Monterey, CA, 2005.

[4] B. Garcia, "Indium Gallium Nitride Multijunction Solar Cell Simulation Using Silvaco ATLAS," M.S. thesis, Naval Postgraduate School, Monterey, CA, 2007.

[5] C. R. Nave. (2010). HyperPhysics. [Online]. Available: http://hyperphysics.phy-astr.gsu.edu/hbase/hframe.html

[6] M. Niaz *et al.* (2010, Jan.) Reconstruction of the History of the Photoelectric Effect and its Implications for General Physics Textbooks. *Sci Ed* [Online] vol. 94, pp. 903-931. Available: http://onlinelibrary.wiley.com/doi/10.1002/sce.20389/full

[7] R. Nelson, "A brief history of thermophotovoltaic development," *Semicond. Sci. Technol.*, vol. 18, pp. 141-143, 2003.

[8] T. Matsuoka *et al.*, "Optical bandgap energy of wurtzite InN," *Appl. Phys. Lett.*, vol. 81, no. 7, pp. 1246-1248, Aug. 2002.

[9] C. Caetano *et al.*, "Theoretical support for the smaller band gap bowing in wurtzite InGaN alloys," in *28th Int. Conf. Physics Semiconductors*, pp. 257-258, 2007.

[10] J. Ager and W. Walukiewicz, "High efficiency, radiation-hard solar cells," Lawrence Berkeley Nat. Lab., Berkeley, CA, LBNL Rep. 56326, 2004.

[11] *ATLAS User's Manual*, SILVACO, Inc., Santa Clara, CA, 2010.

[12] A. K. Hyder *et al.*, "Static Energy Conversion" in *Spacecraft Power Technologies*, London, U.K.: Imperial College Press, ch. 6, sec. 5, pp. 311-318, 2000.

[13] H. F. Yang *et al.*, "Optical constants of InN thin films on (111) GaAs grown by reactive magnetron sputtering," *J. Appl. Phys.*, vol. 91, no. 12, pp. 9803-9808, Jun. 2002.

[14] R. Goldhahn *et al.*, “Dielectric function of “narrow” band gap InN,” in *Mat. Re. Soc. Symp. Proc.*, pp. 361-368, 2003.

[15] GATS, Inc. (2007). Calculation of Blackbody Radiance. [Online]. Available: http://spectralcalc.com/blackbody/blackbody.html.

INITIAL DISTRIBUTION LIST

1. Defense Technical Information Center
   Ft. Belvoir, VA

2. Dudley Knox Library
   Naval Postgraduate School
   Monterey, CA

3. Clark Robertson
   Naval Postgraduate School
   Monterey, CA

4. Sherif Michael
   Naval Postgraduate School
   Monterey, CA

5. Todd Weatherford
   Naval Postgraduate School
   Monterey, CA

6. Stephen Bell
   Naval Reactors
   Washington, DC

7. John Howard
   Naval Postgraduate School
   Monterey, CA

8. Michael Howard
   Greensboro, NC

9. Anne Webster
   Lexington, KY

10. Greg Shorr
    Albuquerque, NM

11. Kathleen Haynes
    Park City, UT